

PULSE COMPRESSION IN D3MON RADAR

by

Laura Catalina Rojas Benítez

*Final thesis projet
for the degree of
Engineering degree
and
Master of science in Electronic Engineering*



*SICOM-3rd year
PHELMA Grenoble INP*



*3rd Faculty of Engineering
Politecnico di Torino*

Helsinki, August 2011



UNIVERSITY OF HELSINKI

PROJECT DEVELOPPED AT
*Department of Physics. Division of Atmospheric Sciences
University of Helsinki*

UNDER THE SUPERVISION OF
*Dr. Dmitri Moisseev
dmitri.moisseev@helsinki.fi*

*P.O. Box 48 (Erik Palmenin Aukio 1), 00014 Helsinki, Finland
Ph: +358 9 191 50866, Fax: +358 9 191 50860*

Summary

D3MON radar system is a high frequency, full scan and transportable meteorological radar which uses solid state transmitters. The presence of these transmitters means low peak powers which by using the traditional narrow pulses for the transmission will generate losses in the signal to noise ratio at the output of the radar making it obsolete for meteorological applications.

Nevertheless the use of narrow pulse in radar has a big advantage in matter of resolution. So the idea was then the use of pulse compression, which is a technique that having the advantages of using a short pulse will keep high the signal to noise ratio.

Many pulse compression techniques have been studying during the years for military and meteorological radar applications. The main goal of this project was to study the different pulse compression systems and to choose the one that assure the best performance for D3MOM radar system taking into account the specification of the system and more specifically the specifications for the transmitter and the receiver.

After a careful study of the traditional pulse compression techniques and the integration of different signal processing concepts a complete compression system is proposed.

The compression system consist of a waveform made up by weighted sub-pulses, with specific frequency modulation characteristics, and a compression matched filter that responds to the characteristics of the transmitted waveform.

Résumé

Le D3MON est un système de radar transportable avec un scan complet qui travaille à des fréquences élevées et qui utilise des émetteurs d'état solide. La présence de ces émetteurs signifie des faibles puissances de crête qui en utilisant des traditionnelles impulsions étroites pour la transmission va générer des pertes dans le rapport signal sur bruit à la sortie du radar et les rend obsolète pour des applications météorologiques.

Néanmoins l'utilisation d'impulsions étroites dans le radar a un gros avantage en matière de résolution. Donc l'idée était alors l'utilisation de la compression d'impulsion, qui est une technique que en ayant les avantages d'utiliser une courte impulsion gardera haute le rapport signal sur bruit.

De nombreuses techniques de compression d'impulsion ont été étudié pendant des années pour des applications radars militaires et météorologiques. L'objectif principal de ce projet était d'étudier les différents systèmes de compression d'impulsion et de choisir celui qui assure le meilleur rendement pour le système de radar D3MOM en tenant compte de la spécification du système et plus précisément les spécifications pour l'émetteur et le récepteur.

Après d'une étude approfondie des techniques traditionnelles de compression d'impulsion et de l'intégration des différents concepts de traitement du signal un système de compression complet est proposé.

Le système de compression se compose d'un signal constitué par les sous-impulsions pondérées, avec des précises caractéristiques de modulation de fréquence, et un filtre de compression adapté qui répond aux caractéristiques de l'onde transmise.

Acknowledgements

I am heartily thankful to my supervisor in University of Helsinki, Dr. Dmitri Moisseev, who give the opportunity to work in this project. Whose encouragement, guidance and support from the beginning to the end enabled me to develop the subject and to fall in love with the subject.

It is a pleasure to thank Prof. Laurent Ross from PHELMA and Dr. Riccardo Notarprieto from Politecnico di Torino, for their long distance support, their feedback and all the aide with the administrative issues in France and in Italy.

I would like to thank Matti Leskinen, for his company at the radar laboratory and all the interesting and full of content talks. I would like to show my gratitude to my friend and colleague Diego Angulo. He has made available his support in a number of ways along my master studies.

I am indebted to many of my SICOM colleagues to support me in the hard but amazing learning process I had in France. I owe my deepest gratitude to all my friends in Grenoble for make my exchange year one of the best years of my life, for give me the oportunity to see different ways of thinking and for encourage me to make my dreams come true.

I would like to thank also all the people who I got to spend time with in Italy, for their support and friendship.

Obviously, I would like to thank all my friends and family in Colombia, with whom I have been going through all this process, for their company and advises in despite of the distance.

Finally, I would like to offer the most special thanks to:

My mother, Nelsy Janneth; and my brothers, Miguel and Leonardo, for teaching me the value of the family, for being my example of life, for showing me during my entire life their love and support in all my desicions.

My love, Torsti, for the correction of the paper, for giving me each passing day the reason to believe that everything is possible, for encougaring me in being a better person, for making me belive in myself and stand by me during all this time and make my life happy.

*Laura Catalina Rojas B
September 2011. Helsinki. Finland*

Contents

1	Context	1
1.1	Research Environment	1
1.1.1	Helsinki University	1
1.1.2	Division of atmospheric science	2
1.1.3	Radar research group	2
1.2	Problem statement	3
1.2.1	Three Frequency solid state weather radar (D3MON)	3
1.2.2	The aim	4
1.3	Planning	4
1.3.1	Tasks	4
1.3.2	Gantt Chart	4
1.4	Thesis structure	5
2	Theoretical Framework	6
2.1	Radar generalities	6
2.1.1	General block diagram	6
2.1.2	Waveform	8
2.1.3	Radar frequency	8
2.2	Weather radar signals	8
2.2.1	Weather Radar equation	10
2.3	Matched filter and ambiguity function	11
2.3.1	Matched filter	11
2.3.2	Ambiguity function	14
2.4	Pulse Compression in radar signals	15
2.4.1	Linear frequency modulated pulse	17
2.4.2	Pulse compression by binary phase codes	18
2.5	Related work	20
3	Pulse Compression features	21
3.1	Radar signal simulation	21
3.2	Simulation Block Diagram	23
3.3	Parameters to evaluate	23
3.3.1	Radar sensitivity	23
3.3.2	Radar Resolution	24
3.3.3	Range sidelobes and weighting	26
3.4	Pulse compression system	26
3.4.1	Reducing sidelobes	27
3.4.2	Transmitted signal design	28

4	The high frequency radar (D3MON)	36
4.1	Generalities	36
4.1.1	Radar specifications	36
4.2	Range resolution	38
4.3	Frequency diversity principle	38
4.4	The best choice	39
4.4.1	Deciding number of pulses	40
4.4.2	Changing the values of Bandwidth for each pulse	41
4.5	Proposed pulse compression system	42
4.5.1	Evaluation	45
5	Discussion and recommendations	46
5.1	Conclusions	46
5.2	Future work	47
5.3	Critical analysis of the research	47
A	Range resolutions constants	49
B	Taylor coefficients	51
C	Zac transform of the transmitted signal	52
D	Networks and radar signals	53
D.1	Analytic radar signal	53
D.2	Networks	54

List of Figures

1.1	<i>Gantt Chart</i>	5
2.1	<i>Block diagram for a basic form of radar</i>	6
2.2	<i>Kumpula C-band weather radar (KUM)</i>	7
2.3	<i>Block diagram for Single-antenna radar</i>	7
2.4	<i>Pulsed radar transmitted signal $s(t)$</i>	8
2.5	<i>Ideal scattering example</i>	10
2.6	<i>Analytic filter</i>	11
2.7	<i>Matched filter in time domain</i>	13
2.8	<i>Matched filter implementation</i>	14
2.9	<i>Single pulse ambiguity function</i>	15
2.10	<i>Pulse compression block diagram</i>	16
2.11	<i>Linear Frequency modulated waveform</i>	17
2.12	<i>Linear Frequency modulated signal ambiguity function</i>	18
2.13	<i>Phased-coded transmitted signal</i>	19
2.14	<i>Binary phased-coded signal ambiguity function</i>	20
3.1	<i>Distribution properties of the simulated radar signal</i>	22
3.2	<i>Simulation block diagram</i>	23
3.3	<i>Radar Sensitivity</i>	24
3.4	<i>Range resolution vs Bandwidth</i>	25
3.5	<i>Range resolution</i>	25
3.6	<i>Pulse compression system using LFM</i>	27
3.7	<i>Windowing</i>	28
3.8	<i>Pulse compression system using LFM</i>	29
3.9	<i>Compressed pulse using barker and Golay codes</i>	30
3.10	<i>NLFM waveform design</i>	31
3.11	<i>Power—n cosine spectrum</i>	32
3.12	<i>Frequency and phase characteristics of Zac transform based waveform</i>	34
3.13	<i>Matched filter output for Zac transform based waveform with and without weighting</i>	34
4.1	<i>D3MON general block diagram</i>	37
4.2	<i>Minimum reflectivity caused by the use of combination of pulses</i>	39
4.3	<i>Complex envelope of transmitted pulse with sub-pulses</i>	39
4.4	<i>Simulation scheme when transmitted waveform is a set of sub-pulses</i>	40
4.5	<i>Sensitivity curve for a waveform built up with 2 and 3 pulses</i>	41
4.6	<i>Sensitivity curve changing values of $B2$</i>	42

4.7	<i>Trasnmitted pulse envelope</i>	43
4.8	<i>Transmitted pulse ambiguity function</i>	43
4.9	<i>Frequency characteristic of the trasnmitted pulse</i>	44
4.10	<i>Simulation scheme when transmitted waveform is a set of sub-pulses</i>	44
4.11	<i>Matched filters frequency response</i>	45
4.12	<i>Input and output profile using the proposed compression system</i>	45
A.1	<i>Ambiguity function cut</i>	49
D.1	<i>Spectrum of pulsed radar transmitted signal</i>	53
D.2	<i>Spectrum of pulsed radar analytic transmitted signal</i>	53
D.3	<i>Signals and networks</i>	54

List of Tables

1.1	<i>D3MON schedule</i>	3
2.1	<i>IEEE Standard letter designation for radar frequency bands</i>	9
2.2	<i>Existing Barker codes</i>	19
3.1	<i>Golay codes</i>	29
3.2	<i>PSL values for cosine-squared on pedestral spectrum</i>	33
3.3	<i>PSL values for tangent based waveform</i>	33
4.1	<i>D3MON specifications</i>	37
4.2	<i>Transmitter and receiver specifications</i>	38
4.3	<i>PSL and ISL values for compressed pulse using 2 and 3 pulses in the transmitted waveform</i>	40
4.4	<i>PSL for compressed pulse 3 pulses in the transmitted waveform changing the bandwidth of the pulses</i>	42

Chapter 1

Context

1.1 Research Environment

1.1.1 Helsinki University

The University of Helsinki (UH) was founded in 1640 and since then the university has played an important role in the country.

At the moment the UH is one of the best multidisciplinary research universities in the world. The high-quality research carried out by the university creates new knowledge for educating diverse specialists in various fields, and for utilization in social decision-making and the business sector.

The university, with almost 4,000 researchers and teachers, operates on four campuses in Helsinki and at 17 other locations. There are 35,000 students, and a further 30,000 participate in adult education.

Founded in 1640, the University of Helsinki wants to strengthen its position among the world's leading multidisciplinary research universities and to actively promote the well-being of humanity and a fair society. Within its main tasks are:

1. Research: The main goal of all the research programs at the University of Helsinki is high quality and good international standards in the different fields. The University puts great effort into promoting the status of basic research in the society being thus coherent with the mission of the League of European Research Universities.
2. Education: The university provides training in about 300 subjects and study programs. There are 35,000 degree students. Approximately 4,500 Master's degree students and about 500 Doctorates are carried out each year.

The quality in the education programs at the University of Helsinki is qualified high on a European level, according to an international assessment. The UH continuously develops teaching and study advising. The university performs multidisciplinary learning research, and the teachers have good resources for learning the latest applications in university pedagogy and using ICT for teaching.

3. Social integration: The UH takes social responsibility, advocates science, and is a recognized partner for cooperation. A short term plan in the university is to intensify its interaction with the society thus clarifying its social responsibility, developing leadership and in longer term specifying its interest group policy.

1.1.2 Division of atmospheric science

Atmospheric sciences relate to all the physical, meteorological and chemical processes that take place in the atmosphere.

The Division of Atmospheric Sciences belongs to the Physics Department of the Science Faculty at Helsinki University. The division of atmospheric sciences centers its efforts in the study of the following topics:

1. Atmospheric aerosols: In this field, the main idea is to study climate variations and the health implications that those changes carry with them.
2. Micro meteorology: The principal studies are about the interactions of different ecosystems and the atmosphere and the carbon sinks.
3. Meteorological modeling: Within this topic the division is working on climate and Martian gas sphere research as well as the development of weather forecast models.
4. Weather radar: The division relies on its own source of radar measurements Kumpula C-band weather radar (KUM) which is a Vaisala¹ Weather Radar prototype.

The division has many links with all kinds of organizations, societies, universities and research networks in national, Nordic-Baltic, European and global level which give it a wide source of information and interaction with the recent research done in all the interest areas.

1.1.3 Radar research group

The radar meteorology group at the University of Helsinki is a multidisciplinary group of researchers who are working on different applications of the weather radar signals: insect detection, precipitation modeling, radar signal processing, etc.

Actual Research

Dual polarization spectral characterization of precipitation A complimentary use of spectral and polarimetric observations provides a new look into cloud and precipitation microphysics.

Doppler observations of separate backscattered signals coming from hydrometeors of different masses and polarimetric measurements can be used to identify those signals.

These observations are being used for rain and ice precipitation microphysical studies.

¹Finnish global leader in environmental and industrial measurement and services for meteorology

Radar signal processing Ground clutter is a long-standing problem that limits use of weather radar observations. The spectral decompositions of differential reflectivity, differential phase and co-polar correlation coefficient are used to discriminate between weather and non-weather signals in spectral domain.

In addition parametric spectral estimation techniques are used for this purpose.

Advanced radar applications This research is part of a research program called Measurement, Monitoring and Environmental Assessment (MMEA) driven by the Finnish Energy and Environment Strategic Center (CLEEN Ltd). The main goal of this project is to develop new tools, standards and methods for environmental measurement, monitoring and decision support, which are attractive to both national and international markets. The idea is to work in different packages. The specific objective for the UH radar group is to participate actively in creating a new package which develops new remote sensing technologies and applications and at the same time integrates them in an interoperable measurement systems and management system for environmental efficiency. Two tasks within this package: advanced mobile high frequency radar and advanced algorithms for weather radars, are the main interests in the ongoing research at the radar group.

1.2 Problem statement

1.2.1 Three Frequency solid state weather radar (D3MON)

The D3MON high frequency radar is three frequency, full scan and transportable radar (Ku (10.95 to 14.5GHz), Ka (26.5 to 40GHz), and W (75 to 110GHz) bands). Its main characteristic is that the radar uses solid state transmitters which means that an arbitrary signal generation is required.

In order to organize the work the radar group made a 5-year schedule which is summarized in table 1.1.

D3MON Schedule	
Year	Activities
1 st	System specifications and preliminary design
2 nd	Detailed design with component level and software module testing, Simulator development
3 rd	Detailed design continued, prototype manufacturing and testing
4 th	Demonstrator radar manufacturing and integration
5 th	Application demonstrations

Table 1.1: *D3MON schedule*

At this moment the project is starting the 2nd year

1.2.2 The aim

The use of solid-state transmitters in radar applications will generate losses in the radar's sensitivity if the system uses the conventional narrow pulses for the transmission. This is due to the low peak powers of the transmitters.

In order to solve the problem of the sensitivity the idea is to use pulse compression waveforms, but that means that during the transmission of the long pulse the receiver is not going to receive any signal, so the idea is to solve this by staggering frequency modulated short and long pulses .

The goal of the research is then to choose the proper combination of modulation-filter for those pulses in order to achieve the best performance possible.

The simulations were done in Matlab, some codes were provided.

1.3 Planning

1.3.1 Tasks

1. Documentation of weather radar signals, doppler weather radars, matched filter and ambiguity function, frequency and phase modulation and pulse compression.
2. To simulate radar signals in range and sample times using the code provided taking into account that the power of the signal in the range time will vary depending on a measured reflectivity profile input from real radar observations.
3. To implement the convolution of the simulated signal with different transmitted waveforms and pass the result through an adequately designed matched filter starting with simple waveform i.e. rectangular pulse.
4. To implement the mismatched filter in order to achieve side lobes suppression with power conservation for each one of the proposed waveforms designed in the previous stage.
5. The final step of the project is to find optimum waveform-filter combination with the following characteristics: Integrated side lobes lower than -50 dB, power conservation increasing the range resolution.

1.3.2 Gantt Chart

In order to organize the development of the thesis a Gantt chart was chosen taking into account the complexity of the different activities. See figure 1.1 on page 5. As shown the tasks proposed in the previous section were divided and scheduled in the different phases.

It is important to mention that at the beginning of each activity one week was set to the research of specific information about the topic of interest for making the activities and their challenges clear. The simulations include provided and created codes, which helped in the theoretical verification and the validation of the proposal.

The writing activity started from the 5th week and it also implied learning how to use \LaTeX .

Month	March				April				May				June				July				August							
Week	1	2	3	4	1	2	3	4	1	2	3	4	1	2	3	4	1	2	3	4	1	2	3	4				
Documentation	■	■	■	■	■				■	■		■			■				■		■				■			
Radar signal simulations			■	■	■	■	■																					
Matched filter design									■	■	■																	
Mismatched filter design										■	■																	
Analysis waveform-filter													■	■		■	■			■	■		■					
Validation																												
Conclusions																						■	■	■	■	■		
Writing					■	■	■	■	■	■	■	■	■	■	■	■	■	■	■	■	■	■	■	■	■	■		
Oral presentation																								■	■			

Figure 1.1: Gantt Chart

The oral presentation phase includes setting up the slides, the poster and the speech.

The yellow color during 3rd week of June and 3rd week of July correspond to the holiday periods.

1.4 Thesis structure

The final objective of this thesis is to reach the best waveform-filter combination in order to get the best performance of the D3MON radar. For that reason the research is structured in the way that one can have all the information needed in order to make the comparisons pointing out advantages and disadvantages of all considered possibilities. Chapter 2 introduces the fundamental principles of weather radars needed to understand all issues faced in radar signal design; it explains the basic concepts of radar signal processing like pulse compression, matched filter, mismatched filter; and describes some work already done in this field. Chapter 3 presents a detailed study about different pulse compression waveforms and filters to be used in the receiver; puts forward comparison between the different solutions highlighting advantages and disadvantages for each case, the chapter will provide the main elements to build the solution for the D3MOM radar. Chapter 4 exhibits the specifications of the system, the proposed solution and its validation. Finally chapter 5 comes up with the conclusions, the critical analysis about the work and exposes some of the further work that can be done in pulse compression in weather radar field.

Chapter 2

Theoretical Framework

2.1 Radar generalities

The word radar comes from the acronym: **R**Adio **D**etection **A**nd **R**anging. Radar is an object-detection system which uses electromagnetic waves to measure range, altitude, direction or speed of moving and fixed objects like airplanes, ships, cars, meteorological phenomenon, and even the ground.

Radar operation starts in the transmitter with the emission of pulses, in radio waves or microwaves, which propagate in space. When the pulses find a reflecting object some part of the energy of the wave is returned or scattered to the receiver. The reflected waves are usually called *echoes* and contain both the energy of the desirable reflecting objects, or *targets*, and the energy of the undesirable reflecting objects or *clutters*.

Once the echoes are received the next step is to decide whether it corresponds or not to a target, which is done using a proper signal processing in the receiver, having at the same time additional information about the target for example: location, speed, dimensions, etc.

2.1.1 General block diagram

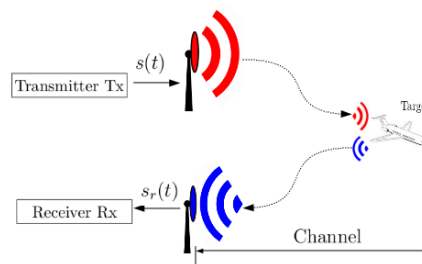


Figure 2.1: *Block diagram for a basic form of radar*

Figure 2.1 shows the basic diagram of a radar system. A basic radar system consist of 3 blocks: transmitter, receiver and antennas. The target is part of

the propagation medium, or *channel* between the transmission and reception of the waves.

The antenna is an electrical device which couples waves in a free space to an electrical current that is going to be used by the receiver or the transmitter. In radars the antenna allows the transmitted electromagnetic waves to propagate in the space and collects the echoes, it has also some filtering properties that can be used in order to improve some features.

The antenna is usually an elliptic paraboloid and is illuminated by a source located at the focal point. Figure 2.2 is an example of this type of antenna.



Figure 2.2: *Kumpula C-band weather radar (KUM)*

Antenna at Helsinki University .The reflector is a Center fed parabolic reflector, has a diameter of 4.20 m, has a Beamwidth of 1.05 deg with gain of approximately 44.5 dB, feed is corrugated horn with OMT, Horizontal or Simultaneous(SHV) polarization.

In most of the cases the same antenna can be used for transmitting and receiving, in this case a switch selector is needed as in figure 2.3. The function of this multiplexor is to protect the receiver while the transmitter is on and to direct the waves of the echoes to the receiver rather than to the transmitter.

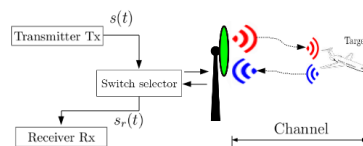


Figure 2.3: *Block diagram for Single-antenna radar*

The transmitter generates an appropriated pulse waveform which, looking for better performance, varies depending on the application. The most common waveform used in radar is a short pulse.

The receiver amplifies the echoes, which usually are weak signals, to levels that allow to detect their presence. It is important to guarantee that the receiver produces as little noise on its own as possible. In order to avoid saturation in the receiver due to the clutters the dynamic range of the receiver should be large enough. Two important processes take place in the receiver: signal processing and detection. Signal processing includes classification of targets and clutters, matched filter, Doppler processing and separation of moving targets.

Detection takes place at the output of the receiver and depends on whether the receiver's output is greater than an established threshold or not. The value of the threshold has to be so that it produces an acceptable rate of false alarms due to the noise in the receiver. Once the detection is performed different information about the target can be obtained.

2.1.2 Waveform

At the output of the transmitter the signal $s(t)$ is defined as in equation 2.1

$$s(t) = a(t) \cos(\omega_0 t + \theta(t) + \phi_0) \quad -\infty < t < +\infty \quad (2.1)$$

where $a(t)$, and $\theta(t)$ correspond respectively to the amplitude and frequency modulation; ω_0 is the operation frequency and ϕ_0 is the phase angle.

In the specific case of the pulsed radar the signal $s(t)$ is defined in finite interval of time. Figure 2.4 shows a transmitted waveform that uses rectangular pulses of duration τ occurring each time that the pulse repetition interval PRT is reached.

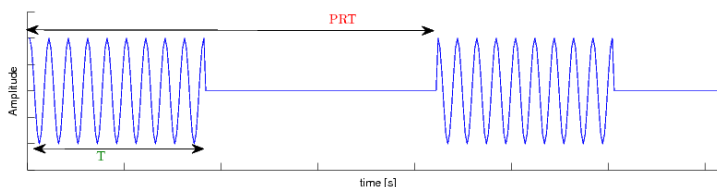


Figure 2.4: Pulsed radar transmitted signal $s(t)$

2.1.3 Radar frequency

The electromagnetic spectrum is the electromagnetic radiation division according to frequency. The electromagnetic spectrum goes from low frequencies, long wavelengths and low energy waves to high frequencies, short wavelengths and high energy waves. The part of the spectrum where the radar works goes from 3MHz to 300GHz . Table 2.1 on page 9 shows the IEEE Standard letter designation for radar frequency bands established initially in 1976 and reviewed and reaffirmed in 1984 [2].

The frequency is chosen depending on the requirements of each system and its applications. Sometimes factors like atmospheric noise, size of the antenna and cosmic noise can constrain the choice of the frequency but at the end the decision is related to the radar mission.

2.2 Weather radar signals

Radar applications in which detection of objects is the main goal the echoes that come from rain, snow, birds and wind are considered clutters. Quite the opposite for meteorological applications these 'clutters' are sources of information and because of this they become the targets.

Band Designation	Frequency Range
<i>HF</i>	3 – 30MHz
<i>VHF</i>	30 – 300MHz
<i>UHF</i>	300 – 1000MHz
<i>L</i>	1 – 2GHz
<i>S</i>	2 – 4GHz
<i>C</i>	4 – 8GHz
<i>X</i>	8 – 12GHz
<i>K_u</i>	12 – 18GHz
<i>K</i>	18 – 27GHz
<i>K_a</i>	27 – 40GHz
<i>V</i>	40 – 75GHz
<i>W</i>	75 – 110GHz
<i>mm</i>	110 – 300GHz

Table 2.1: *IEEE Standard letter designation for radar frequency bands*
In some cases V and W bands are considered in the mm band at frequencies above 40GHz

A weather signal can be understood ultimately as a collection of echoes from a large number of targets. These echoes are received continuously by the receiver where the received signal $S_r(t)$ is a scaled replica of the transmitted signal $S(t)$ shifted in time by the range-time delay t_d and shifted in frequency by the Doppler angular frequency w_d .

The signal $S(t)$ in equation 2.1 can be expressed as well as

$$S(t) = \frac{a(t)}{2} \left(e^{i(w_o t + \theta(t) + \phi_o)} + e^{-i(w_o t + \theta(t) + \phi_o)} \right) \quad (2.2)$$

Using the same form as in equation 2.2 the received signal $S_r(t)$ is as follows:

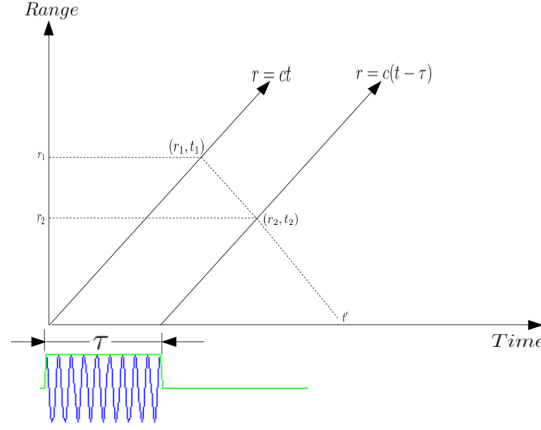
$$S_r(t) = AS(t - t_d)e^{iw_d(t - t_d)} \quad (2.3)$$

$$S_r(t) = A \left(e^{i((w_d + w_o)(t - t_d) + \theta(t - t_d) + \phi_o)} + e^{-i((w_d + w_o)(t - t_d) + \theta(t - t_d) + \phi_o)} \right) \quad (2.4)$$

Where A corresponds to the scattering amplitude including the amplitude modulation and can vary with time. Figure 2.5 on page 10 illustrates how any change in the scattering amplitude influences the received signal through an ideal case where two particles located in two different points r_1 and r_2 with different time-varying amplitudes interact with the rectangular transmitted pulse.

The diagram is a range vs time plot. The line $r = ct$ represents the propagation of the first edge of the transmitted pulse, while the propagation of the other end is represented by the line $r = c(t - \tau)$ where τ is the width of the transmitted pulse. If one wants to see the reflected signal at t' , which is over the line with slope $m = -c$, the contributions from both particle at r_1 and particle at r_2 have to be considered. The contributions are evaluated at $t_i = t' - r_i/c$.

In general the back scatter from the precipitation particles contains a large number of echoes which correspond to particles with different scattering amplitudes and which are moving with different velocities and the resultant contribution will be a discrete sum of the contribution from all the particles present in the channel. [3]

Figure 2.5: *Ideal scattering example*

2.2.1 Weather Radar equation

The radar equation represents the relation between the characteristics of the radar, the scatterers, and the received signal.

The antenna, with gain $G(\theta, \phi) = G_o f(\theta, \phi)$ where $f(\theta, \phi)$ is the normalizer power antenna's pattern, transmits the power P_t generated in the transmitter.

At the scatterer the power density is reduced by a factor of $\frac{1}{4\pi r^2}$, due to the reflected wave's travel over a distance r . The power density at the scatterer is then $\frac{P_t G}{4\pi r^2}$. In weather radar applications it is reasonable to assume that the magnitude square of the time-varying scattering amplitude is stationary and because of that the total power intercepted by the scatterer is related to the sum of the radar cross sections σ of all the scatterers in the channel.

Considering the reflectivity $n(r, \theta, \phi)$ as the average radar cross section per unit volume [3] the mean power at the receiver P_r is

$$P_r = \left(\frac{\lambda^2 P_t G_o}{4\pi^3} \right) \int_V \frac{f^2(\theta, \phi)}{r^4} \eta(r, \theta, \phi) |a(t - \tau)|^2 dV \quad (2.5)$$

If the transmitted signal is a rectangular pulse of width τ and normalizing the radar cross section per unit of volume the mean power at the receiver in equation 2.5 will be:

$$P_r = \left(\frac{\lambda^2 P_t G_o}{4\pi^3 r_o^2} \right) \frac{c\tau}{2} \iint f^2(\theta, \phi) \eta(r_o, \theta, \phi) d\Omega \quad (2.6)$$

Where r_o corresponds to the center of the transmitted pulse. Equation 2.6 yields the result that the signal power received at time t' is due to the particles of the precipitation in the resolution volume located at distance r .

Typically pencil-beam antennas are used in weather radar. So according to the Probert-Jones approximation for narrow beam antennas, the double integral in equation 2.6 is reduced to

$$\iint f^2(\theta, \phi) \eta(r_o, \theta, \phi) d\Omega \approx \frac{\pi \theta_1 \phi_1}{8 \ln 2} \quad (2.7)$$

Where θ_1 and ϕ_1 are the $3dB$ beamwidths. Putting together 2.6 and 2.7. The mean power at the receiver becomes

$$\bar{P}_r(r_o) = \left(\frac{c\tau}{2}\right) \left(\frac{P_t G_o^2}{\lambda^2 4\pi^3}\right) \left(\frac{\pi\theta_1\phi_1}{8\ln 2}\right) \left(\frac{\eta(r_o)}{r_o^2}\right) \quad (2.8)$$

The reflectivity $n(r_o)$ can be expressed in terms of the reflectivity factor Z , which depends primarily on the dielectric factor K here the relative permittivity of the water is used because our interest is to work with precipitation

$$|K|^2 = \left|\frac{\varepsilon_r - 1}{\varepsilon_r + 2}\right|^2 \quad (2.9)$$

$$Z = \frac{\lambda^4}{\pi^5 |K|^2} \eta(r_o) \quad (2.10)$$

Replacing 2.10 in 2.8 the radar equation will be defined as the following

$$\bar{P}_r(r_o) = \left(\frac{c\tau}{2}\right) \left(\frac{P_t G_o^2}{\lambda^2 4\pi^3}\right) \left(\frac{\pi\theta_1\phi_1}{8\ln 2}\right) \left(\frac{\pi^5 |K|^2 Z(r_o)}{r_o^2}\right) \quad (2.11)$$

From equation 2.11 it is easy to see that the power at the receiver depends on a meteorological quantity related directly with the reflectivity factor K . Equation 2.11 can be written as

$$\bar{P}_r(r_o) = C\tau \left(\frac{Z(r_o)}{r_o^2}\right) \quad (2.12)$$

Where C is the constant related to the radar.

2.3 Matched filter and ambiguity function

2.3.1 Matched filter

Considering a pulse received from a target it is well known that noise is always going to be present. So the idea is to find a particular optimum filter which maximizes the instantaneous signal to noise ratio at the output of the filter. This can be achieved by matching the radar receiver transfer function to the received signal. In a pulsed radar the problem is reduced to finding the impulse response of the filter that maximizes this quantity. In order to do so the problem is simplified as depicted in figure 2.6

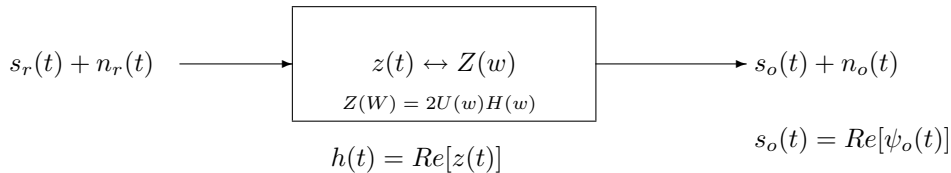


Figure 2.6: *Analytic filter*

The analytical received signal $\psi_r(t)$ with Fourier transformation $\Psi_r(w)$ of the real signal $s_r(t)$ going through the analytic filter ¹ causes a real response $s_o(t)$ whose analytic signal $\psi_o(t)$ is given by equation 2.13, where $\Psi_o(w)$ is the Fourier transformation of $\psi_o(t)$.

$$\psi_o(t) = \frac{1}{2}\psi(t) * z(t) = \frac{1}{2\pi} \int_{-\infty}^{+\infty} \frac{1}{2}\Psi_r(w)Z(w)e^{jw t} dw \quad (2.13)$$

Defining t_o as the time at which the optimum response takes place the peak output signal power \widehat{S}_o will be

$$\widehat{S}_o = |\psi_o(t_o)|^2 = \frac{1}{4} \left| \frac{1}{2\pi} \int_{-\infty}^{+\infty} \Psi_r(w)Z(w)e^{jw t_o} dw \right|^2 \quad (2.14)$$

Considering just as the input the noise $n_r(t)$ with spectrum $N_r(w)$ the power spectrum at the output will be the multiplication of the impulse response of the magnitude square of real filter in frequency by the spectrum of the noise. The average output noise power N_o in terms of the transfer function of the analytic filter is

$$N_o = \frac{1}{4\pi} \int_{-\infty}^{+\infty} N_r(w)|Z(w)|^2 dw \quad (2.15)$$

The idea then is to maximize the ratio $\frac{\widehat{S}_o}{N_o}$

$$\frac{\widehat{S}_o}{N_o} = \frac{\frac{1}{4} \left| \frac{1}{2\pi} \int_{-\infty}^{+\infty} \Psi_r(w)Z(w)e^{jw t_o} dw \right|^2}{\frac{1}{4\pi} \int_{-\infty}^{+\infty} N_r(w)|Z(w)|^2 dw} \quad (2.16)$$

Using Schwarz's inequality 2.17 that is only valid if $A(w) = KB(W)$ where K is an arbitrary constant different from zero

$$\left| \int_{-\infty}^{+\infty} A(w)B(w)dw \right|^2 \leq \left| \int_{-\infty}^{+\infty} A(w)dw \right|^2 \left| \int_{-\infty}^{+\infty} B(w)dw \right|^2 \quad (2.17)$$

and setting $A(w) = \frac{1}{\sqrt{2\pi}\sqrt{N_r(w)}Z(w)}$ and $B(w) = \frac{1}{\sqrt{2\pi}} \frac{\Psi_r(w)e^{jw t_o}}{\sqrt{N_r(w)}}$

The ratio $\frac{\widehat{S}_o}{N_o}$ which provides the optimum value given by

$$\frac{\widehat{S}_o}{N_o} \leq \frac{1}{4\pi} \int_{-\infty}^{+\infty} \frac{|\Psi_r(w)|^2}{N_r(w)} dw = \left(\frac{\widehat{S}_o}{N_o} \right)_{max} \quad (2.18)$$

and from 2.18 the optimum value for the analytic filter $Z(W)$ is

$$Z(w) = \frac{K\Psi_r^*(w)e^{-jw t_o}}{N_r(w)} \quad (2.19)$$

and the optimum value for the real filter $H(w)$ is

$$H(w) = \frac{K S_r^*(w)e^{-jw t_o}}{N_r(w)} \quad (2.20)$$

¹The different networks and their interaction with the radar signals are explained in Appendix D

where K is the arbitrary constant of the condition in Schwarz's inequality.

Now supposing the case of white noise, that means that the spectrum $N_r(w)$ is a constant equal to $\frac{N_o}{2}$ in all frequencies the optimum in 2.19 and 2.20 are reduced to

$$Z(w) = \frac{2K}{N_o} \Psi_r^*(w) e^{-jw t_o} \quad (2.21)$$

$$H(w) = \frac{2K}{N_o} S_r^*(w) e^{-jw t_o} \quad (2.22)$$

So the optimum value of $\left(\frac{\widehat{S_o}}{N_o}\right)_{max}$ is

$$\left(\frac{\widehat{S_o}}{N_o}\right)_{max} = \frac{1}{N_o 2\pi} \int_{-\infty}^{+\infty} |\Psi_r(w)|^2 dw = \frac{E_{\psi_r}}{N_o} = \frac{2E_r}{N_o} \quad (2.23)$$

Where E_R and E_{ψ_r} are the energies of $S(t)$ and $\Psi_r(t)$, respectively.

Considering the specific case of the radar where each target has a range delay T_d and taking into account the properties of the radar through C , the constant of the Radar in the radar equation 2.12, the signal at the receiver $s_r(t)$ can be written as the following

$$S_r(w) = CS(W) e^{-jw t_d} \leftrightarrow s_r(t) = Cs(t - T_d) \quad (2.24)$$

and the analytic signal at the receiver $\psi_r(t)$ is written as

$$\Psi_r(w) = C\Psi(W) e^{-jw t_d} \leftrightarrow \psi_r(t) = C\psi_r(t - T_d) \quad (2.25)$$

Using 2.21 and 2.22 into 2.25 and 2.24 respectively the impulse response for the filter become

$$Z(w) = \frac{2KC}{N_o} \Psi_r^*(w) e^{-jw(t_o - t_d)} \leftrightarrow z(t) = \frac{2KC}{N_o} \Psi_r^*(t_o - t_d - t) e^{-jw t_o} \quad (2.26)$$

$$H(w) = \frac{2KC}{N_o} S_r^*(w) e^{-jw(t_o - t_d)} \leftrightarrow h(t) = \frac{2KC}{N_o} s_r^*(t_o - t_d - t) e^{-jw t_o} \quad (2.27)$$

Figure 2.7 shows the matched filter in time domain

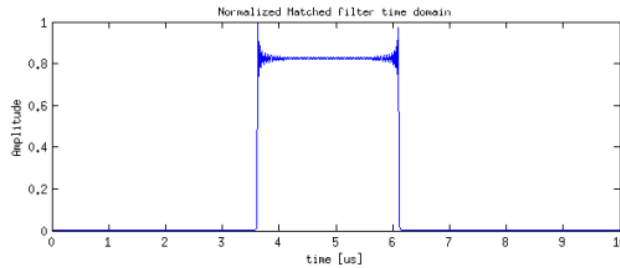


Figure 2.7: Matched filter in time domain

As it is shown in figure 2.7 the transfer function of the matched filter is proportional to the spectrum of the transmitted signal $S_r(w)$ and depends only on the energy of the signal and the noise level as it is shown in equation 2.23. The transfer function of the filter that generates the maximum signal to noise ratio doesn't depend on the shape or modulation of the transmitted signal and removes any phase variation in the spectrum of the input signal.[5]

The matched filter output can be then written as in 2.30

$$\psi_o(t) = \frac{1}{2} \psi_r(t) * z(t) \quad (2.28)$$

$$\psi_o(t) = \frac{1}{2} \int_{-\infty}^{+\infty} \psi_r(t) C \psi_r(t - T_d) \frac{2KC}{N_o} \Psi_r^*(t_o - t_d - t + x) e^{-jw t_o} dx \quad (2.29)$$

$$\psi_o(t) = \frac{KC^2}{N_o} \int_{-\infty}^{+\infty} \psi^*(\zeta) \psi(\zeta + t - T_o) d\zeta \quad (2.30)$$

Figure 2.8 is the implementation of equation 2.30

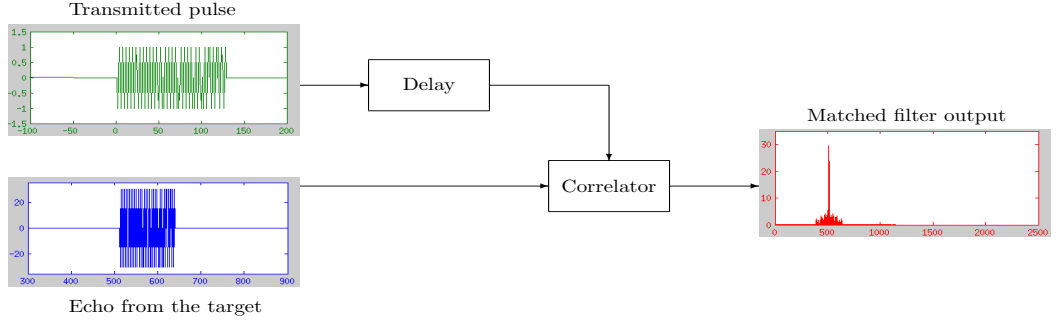


Figure 2.8: Matched filter implementation

2.3.2 Ambiguity function

Considering a moving target and starting from equation 2.4 the analytic signal of $s_r(t)$ is

$$\psi_r(t) = C g(t - t_d) e^{j((w_o + w_d)(t - t_r) + \phi_o)} \quad (2.31)$$

$$\psi_r(t) = C \psi(t - t_d) e^{j((w_o + w_d)(t - t_r))} \quad (2.32)$$

where $g(t - t_d) = a(t - t_d) e^{j\theta(t - t_d)}$ and $\psi(t - t_d) = g(t - t_d) e^{j(w_o(t - t_d) + \phi_o)}$

The idea is then to apply $\psi_r(t)$ to the optimum filter for $\psi(t)$ and then the output $\psi_o(t)$ will be given by the expression

$$\psi_o(t) = \frac{KC^2}{N_o} e^{j(w_o + w_d)(\tau)} \int_{-\infty}^{+\infty} g^*(\xi) g(\xi + \tau) e^{jw_a \xi} d\xi \quad (2.33)$$

The expression $\int_{-\infty}^{+\infty} g^*(\xi) g(\xi + \tau) e^{jw_a \xi} d\xi$ is known for some authors as the matched filter response $\chi(\tau, w_d)$. It completely determines the response to a moving target by the filter when it is matched to a stationary target. The expression $|\chi(\tau, w_d)|^2$ is the Ambiguity function. The principal characteristics of this function are:

1. Its maximum occurs at the origin and it is determined by the total energy contained in the signal.
2. In the plane τ vs w_d first and third quadrants as well as fourth and second follow the symmetry property.
3. The volume is not dependent on the modulation of the signal it is determined by the total energy of the signal.

Figure 2.9 on page 15 show the ambiguity function for a single pulse transmitted signal

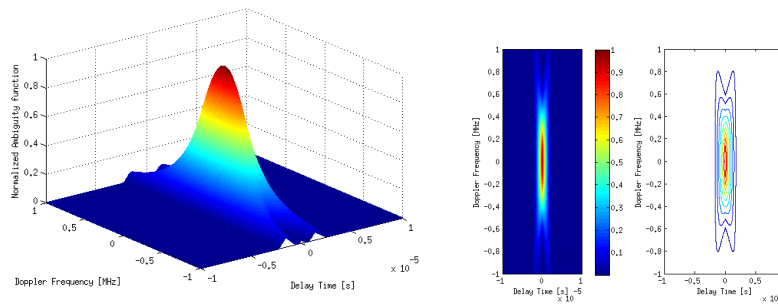


Figure 2.9: *Single pulse ambiguity function*

The ideal ambiguity function is a 2 dimensional delta function that reaches its maximum value at $(0, 0)$ and is zero elsewhere. This ideal function means no ambiguity and it is not physically realisable even though there are some good approximations to it through the modulation of the input signal. It is important to mention that any doppler shift can cause no detection of the targets but with an appropriate doppler processing the ranging can be accurately done.

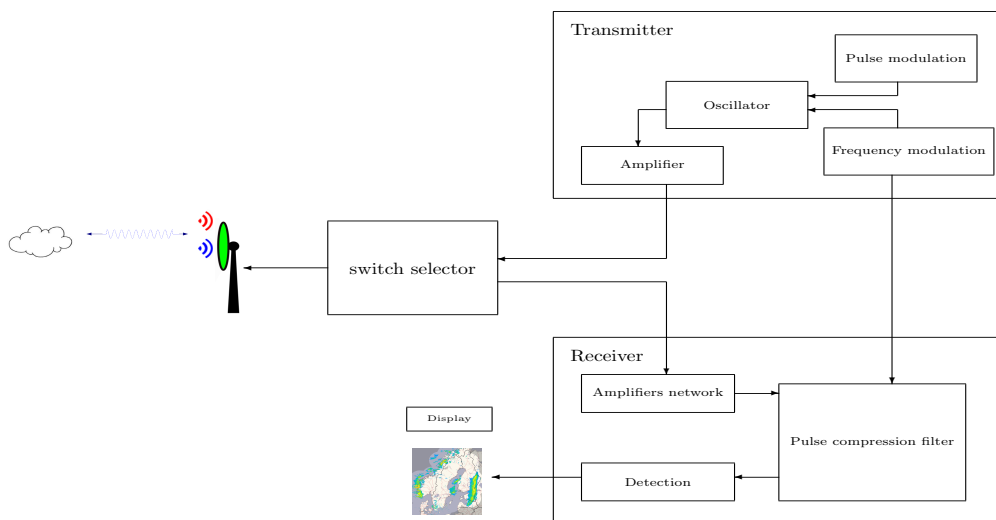
For radar applications the principal task is then to design signals and corresponding ambiguity functions that have good resolution properties in both range and doppler [7]

2.4 Pulse Compression in radar signals

The use of short pulse widths in radar includes within its advantages superior range resolution, which is the ability to distinguish between two or more targets that are close in range, and small blind range, but it also includes losses in the signal to noise ratio. So in order to have the advantages of using a short pulse and at the same time keep the signal to noise ratio as high as it is possible the *Pulse compression* technique is used.

The pulse compression technique achieves the conversion of a long duration pulse into a short effective pulse. This is possible by increasing the bandwidth of the transmitted pulse through the frequency modulation of the pulse and correlating the received signal with the transmitted pulse. Figure 2.10 shows the basic diagram of pulse compression in radar.

Generation of the transmitted pulse takes place in the transmitter through the oscillator's output amplification. The oscillator's output is the result of the

Figure 2.10: *Pulse compression block diagram*

integration between amplitude and frequency modulation of the pulse. The frequency modulation is important in the compression filter design too, because this filter is created to recognise the characteristics of the transmitted pulse, in other words it is matched to the transmitted waveform. In this way the received echoes with similar characteristics to the transmitted waveform will be recognised by the pulse compression filter whereas received echoes without similarities will be ignored by the filter.

Supposing that the compression filter has a bandwidth B , the power noise within the filter is $N_{mf} = N_o B$ and the average input power $\widehat{S}_r = \frac{E_r}{\tau}$, where τ is the width of the pulse. The signal to noise ratio (SNR) at the input of the compression filter is

$$\left(\frac{\widehat{S}_r}{N_{mf}} \right) = \frac{E_r}{N_o B \tau} \quad (2.34)$$

In order to compute the instantaneous output peak SNR to the input SNR ratio equations 2.35 and 2.18 are used

$$\frac{\left(\frac{\widehat{S}_o}{N_o} \right)}{\left(\frac{\widehat{S}_r}{N_{mf}} \right)} = 2B\tau \quad (2.35)$$

Where $B\tau$ is known as the *Pulse compression ratio*. This quantity represents the matched filter gain, so more the received signal is close to the transmitted pulse the more the compression ratio is close to the maximum value $B\tau$.

In the radar equation 2.12 the effect of the pulse compression is showed in

2.36

$$\bar{P}_r(r_o) = C(n\tau_{sp}) \left(\frac{Z(r_o)}{r_o^2} \right) \quad (2.36)$$

Where $n\tau_{sp} = \tau$, this means that the transmitted pulse with width pulse τ can be interpreted as a serie of short pulses with width pulse τ_{sp} and for these reason and as long as the transmitted pulse doesn't change the power at the receiver remains also unchanged no matter the signal bandwidth.

The range resolution, on the contrary, has a inverse proportionality with the signal bandwidth $Res = \frac{c}{2B}$ so keeping the characteristics of the pulse and increasing the bandwidth the range resolution is improved.

Depending on the waveforms used in the generation of the pulse the advantages of pulse compression are enhanced. In the following sections some implementations of pulse compression with different waveforms are described.

2.4.1 Linear frequency modulated pulse

Implementing pulse compression using a linear frequency modulated pulse as the trasmitted signal implies the following changes in the signals through the radar system.

First of all the transmitted signal $s(t)$ consider in 2.1 becomes 2.37 replacing the amplitud modulation term $a(t)$ by $a(t) = Arect\left(\frac{t}{\tau}\right)$ and the frequency modultaion term $\theta(t)$ by the proposed modulation $\theta(t) = \frac{\mu}{2}(t)^2$.

$$s(t) = Arect\left(\frac{t}{\tau}\right) \cos(\omega_0 t + \frac{\mu}{2}(t)^2 + \phi_0) \quad (2.37)$$

The μ term is related with the frequency sweep B and the pulse width τ by $\mu = \frac{B}{\tau}$. the instantaneous frequency $W_i(t)$ due to the frequency modulation is $w_i(t) = \mu t$ between the interval $[-\frac{\tau}{2}, \frac{\tau}{2}]$. Figure 2.11 shows the linear frequency modulated waveform.

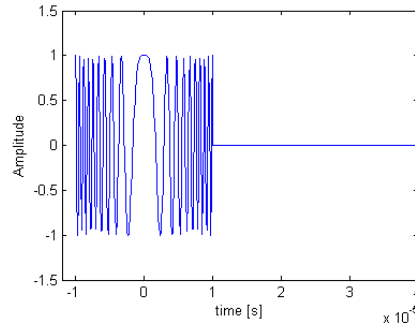


Figure 2.11: *Linear Frequency modulated waveform*

In this case is easy to work with the complex envelope $g(t)$ of the transmitted signal using 2.37 and D.5 the complex envelope $g(t)$ is written as the following

$$g(t) = Arect\left(\frac{t}{\tau}\right) e^{j\frac{\mu t^2}{2}} \quad (2.38)$$

The analytic signal $\psi(t)$ in D.4 becomes

$$\psi(t) = A \operatorname{rect}\left(\frac{t}{\tau}\right) e^{j(w_o t + \frac{\mu t^2}{2} + \phi_o)} \quad (2.39)$$

The analytic received signal ψ_r is given by the expression

$$\psi_r(t) = C \psi(t - t_d) e^{j w_d (t - t_d)} \quad (2.40)$$

$$\psi_r(t) = C = A \operatorname{rect}\left(\frac{t - t_d}{\tau}\right) e^{j((w_o + w_d)(t - t_d) + \frac{\mu(t - t_d)^2}{2} + \phi_o)} \quad (2.41)$$

Considering an analytic matched filter network the signal $\psi_r(t)$ is applied to it and thus the output of the filter will be given by the expression in 2.30 and the function $g(t)$ determines the behaviour of the output of the filter.

$$\psi_o(t) = \frac{K C^2}{N_o} e^{j(w_o + w_d)(\tau)} \int_{-\infty}^{+\infty} g^*(\xi) g(\xi + \tau) e^{j w_d \xi} d\xi \quad (2.42)$$

$$\psi_o(t) = \frac{K C^2}{N_o} e^{j(w_o + w_d)(\tau)} \chi(\tau, w_d) \quad (2.43)$$

Figure 2.12 shows the behaviour of the ambiguity function of this kind of signals.

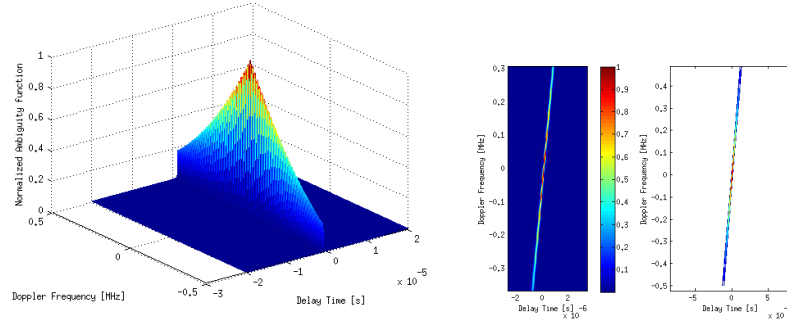


Figure 2.12: *Linear Frequency modulated signal ambiguity function*

As one can appreciate in the figure 2.12 these waveforms have a group delay, which is proportional to the frequency. The ambiguity function consists of a long crest with slope $\frac{B}{\tau}$, its ambiguity function is similar to the single pulse ambiguity function, except that it is cut on the bias in the *timedelay vs doppler frequency* plane. The variations in the doppler frequency seem not to change that much the shape of the pulse and its amplitude is reduced a little but in the other hand the pulse is shifted in time.

2.4.2 Pulse compression by binary phase codes

The implementation of pulse compression by using phase coding is basically done because it is a form to use digital techniques that allows implement the pulse compression with low sidelobes. The radar signals will change as the following:

In order to apply digital techniques the transmitted pulse $s(t)$ with pulse width τ is subdivided in N subpulses with pulse width $\tau_1 = \frac{\tau}{N}$ and keeping the

same carrier frequency for each subpulse the idea is to change the phases from subpulse to subpulse and in this way a *code* is created. The problem now is to choose the appropriated code that allow to have low sidelobes in compression.

Binary phase codes consist of a sequence a_k of either $+1$ or -1 and in this way the phase varies between 0 and π as shown in the figure 2.13.

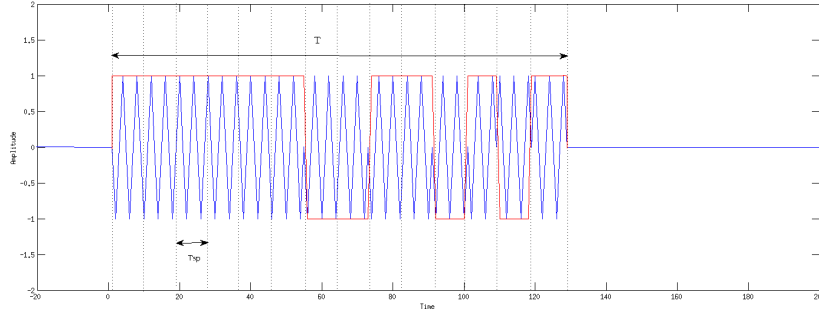


Figure 2.13: *Phased-coded transmitted signal*

The complex envelope $g(t)$ of the transmitted signal can be written as

$$g(t) = A \sum_{k=1}^N a_k \text{rect} \left[\frac{t + \left(\frac{N+1}{2} - k\right) T_{sp}}{T_{sp}} \right] \quad (2.44)$$

In order to have low sidelobes the choice of the code is critical. The optimal binary amplitude sequence is the one whose autocorrelation function has the smallest possible peak sidelobe magnitude. This codes are well-known as *The Barker codes*[6].

A barker code is a sequence b_k of N values of $+1$ or -1 for $K = 1 \dots N$ such that $\left| \sum_{k=1}^{N-a} b_k b_{k+a} \right| \leq 1$ for all $1 \leq a \leq N$, this means that the correlation side lobe is lower or equal to 1

In table 2.2 are listed all known Barker codes and those having a minimum peak sidelobe of 1.

Length	Code
2	+1 -1 +1 +1
3	+1 +1 -1
4	+1 -1 +1 +1 +1 -1 -1 -1
5	+1 +1 +1 -1 +1
7	+1 +1 +1 -1 -1 +1 -1
11	+1 +1 +1 -1 -1 -1 +1 -1 -1 +1 -1
13	+1 +1 +1 +1 +1 -1 -1 +1 +1 -1 +1 -1 +1

Table 2.2: *Existing Barker codes*

As shown in the table 2.2 the longest existing Barker code is $N = 13$.

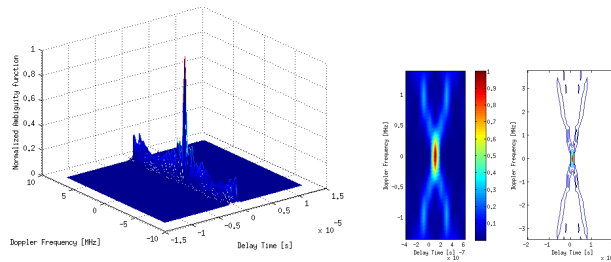


Figure 2.14: *Binary phased-coded signal ambiguity function*

The typical ambiguity function for this type of transmitted signal is shown in figure 2.14 on page 20

As it is evident this ambiguity function has a narrow spike at the center and sidelobes, and in most of the cases presents uniformity.

2.5 Related work

Simulation of dispersed time-varying echoes from targets in weather radar has been developed by Chandrasekar, Brangi and Brockwell [9] where they describes the statistical characteristics of radar returns of a coded waveform from distributed targets.

Pulse compression techniques has been well established in military and airplanes applications since 1950. The concept of pulse compression is explain in detail in several books for instance [5] and [10] where the authors make a deep study of the concept and the basic and typical techniques. The research about the use of pulse compression in weather radars took place in 1970 with Fetter [11] who through the implementation of a 7-bit Barker code demonstrated the use of pulse compression to enhance the radar weather performance. Some years later Gray an Farley [12] investigated quantitatively the use of binary phase-coded pulses in incoherent-scatter observations.

However Keeler and Passarelli [13] were the ones who traced the evolution of signal processing for atmospheric radars. In 1998 Mudukutore, chandrasekar and keeler[8]put together the simulation technique in [9] and data analysis to demonstrate that pulse-compression techniques indeed provide aviable option for faster scanning rates while still retaining good accuracy in the estimates of various para metres that can be measured using a pulsed-Doppler radar. From this moment several techniques have been used in radar in order to implement pulse compression like non linear modulation [23], [22]or polyphase coding [15].

All this techniques are going to be evaluated, in order to choose the best option for the DEMON 3-High frequency radar system.

Chapter 3

Pulse Compression features

3.1 Radar signal simulation

In order to develop the signal processing and the data extraction of the echos from the precipitation the simulation of the signals is necessary because this allows to evaluate the signal processing performance in a controlled environment. Using the simulation algorithm for multivariate proposed by V.Chandrasekar and V.N Bringi in [9] the time series from a simple pulse can be simulated. This method takes into account the distribution properties of the signal, radar reflectivity profile, mean velocity, velocity spectrum width and signal to noise ratio. The echo signals from the precipitation contribute to produce a complex signal whose inphase and quadrature components have a Gaussian distribution with zero mean [8] because the echo is assumed to be stationary. In radar a complex signal is generated for each polarization, for instance in a dual polarized radars the information of inphase and quadrature componetes for horizontal and vertical channels will be available.

The power spectral density for a weather signal radar supposed to be stationary plus a white noise is given by 3.1

$$S(f) = \frac{S}{\sqrt{2\pi\sigma_f^2}} e^{-\frac{(f-\bar{f}_d)^2}{2\sigma_f^2}} + 2N_oT_s \quad (3.1)$$

Where S is the mean signal power, \bar{f}_d is the doppler frequency, σ_f is the spectral width, N_o is the mean white noise power, T_s is the time between samples.

In the specific case of dual polarized radars the in-phase and quadrature components of the complex signals are independent, and once again gaussian and random variable with zero mean. In addition to that the power spectrum is a power weighted distribution of radial velocities of all the echos from the particles in the resolution volume modeled as having gaussian distribution.

The spectral coefficients of a bivariate time series are given by

$$S = \begin{bmatrix} S_H \\ S_V \end{bmatrix} = \begin{bmatrix} I_H + jQ_H \\ I_V + jQ_V \end{bmatrix} \quad (3.2)$$

The spectral density in 3.1 of horizontal H and vertical V channels is given then

by the equation

$$f_{HH,VV}(f) = \frac{S_{H,V}}{\sqrt{2\pi}\sigma_f^2} e^{-\frac{(f-\bar{f}_d)^2}{2\sigma_f^2}} + 2N_oT_s \quad (3.3)$$

Where $S_{H,V}$ is the mean power in the horizontal or vertical polarization. In order to assume the mean velocity to be zero and without losing generality simulating power signals[9] the crosscorrelation between horizontal and vertical channels ρ_{HV} can be assumed to be $\rho_{HV}(n) = \rho_{HH}(n)\rho_{HV}(0)$, where $\rho_{HH}(n)$ is autocorrelation of the signal in the H -channel and $\rho_{HV}(0)$ is the correlation between H -channel and V -channel signals at the same time and so the cross spectrum f_{HV} can be written as $f_{HV}(k) = f_{HH}(k)\rho_{HV}(0) = I_{HV} + jQ_{HV}$.

The covariance matrix $COV_{H,V}$ of the H -channel and V -Channel is the following

$$COV_{H,V} = \begin{bmatrix} f_{HH} & 0 & I_{HV} & Q_{HV} \\ 0 & f_{HH} & -Q_{HV} & I_{HV} \\ I_{HV} & -Q_{HV} & f_{VV} & 0 \\ Q_{HV} & I_{HV} & 0 & f_{VV} \end{bmatrix} \quad (3.4)$$

As the the H -channel and V -Channel signals are independent the covariance matrix $COV_{H,V}$ can be expressed as $COV_{H,V} = LL^T$ and the spectral coefficients in 3.2 are given by $S = XL^T$, where X is matrix made up by 4 independent and identically distributed random variables(iid) distributed $N \sim (0, 1)$. At this point by having the spectral sequences it is easy to have the time series through the inverse Fourier transform.

The simulation algorithm is summarized as the follows[9]:

1. Generate X with 4 iid $N \sim (0, 1)$ vectors.
2. Factor $COV_{H,V}$ using the Cholesky factorization $COV_{H,V} = LL^T$.
3. Compute the random vector $S = XL^T$ and form S_V and S_H .
4. Inverse Fourier transform of the time series

The power squence is the magnitude square of the complex time sequence. Figure 3.1 illustrates the distribution properties of the simulated signal.

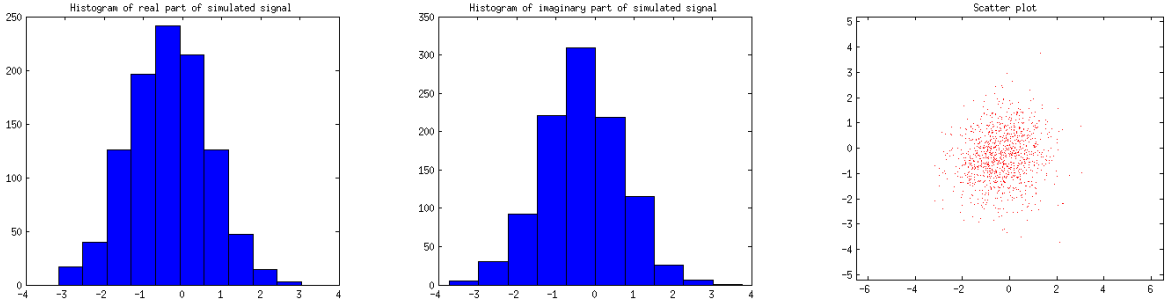


Figure 3.1: *Distribution properties of the simulated radar signal*

3.2 Simulation Block Diagram

In order to decide which kind of waveform is going to be used in the system It was necessary to develop different simulations the block diagram shown in figure 3.2 describes the general scheme used. As it is shown in the diagram the idea is to start from existing measured data from the in-use radar to generate the received signal through the radar signal simulation program developed by Nitin Bharadwaj[16] .

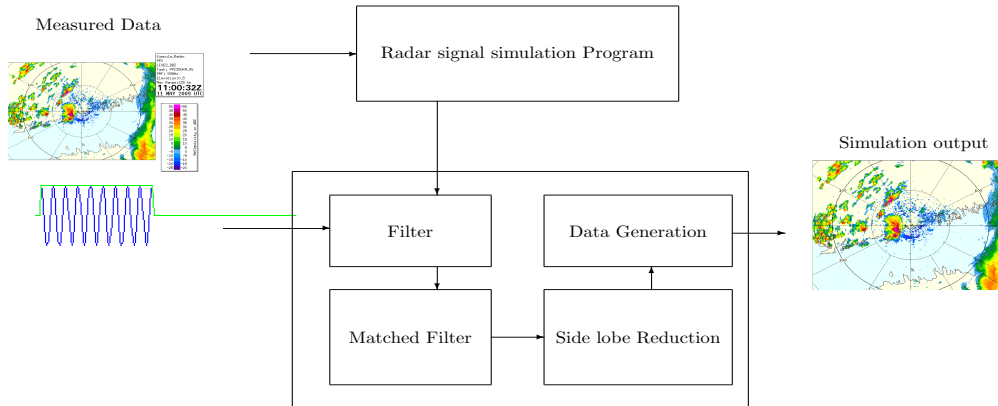


Figure 3.2: *Simulation block diagram*

With the signal produced by the program the idea is to convolve it with the transmitted pulse which is the proposed waveform. Having the convolution of these two signals and in order to use the benefits from the pulse compression a filter, matched to the transmitted pulse, is used. As It was explained in the previous section one of the drawback when one uses pulse compression is the presence of high sidelobes, that in weather observations is a crucial issue. For this reason it is necessary to implement a method that allows to reduce the sidelobes and still gives high performance in matters of power, that means that the main lobe describes well the power content of the received signal .

The final step is to generate the radar returns from the data obtained in the sidelobes reduction block. The idea is to have the most approximated values to the measured data.

3.3 Parameters to evaluate

By implementing any kind of signal processing in the received signal there are three crucial parameters that allow to evaluate the performance of the proposed processing: radar sensitivity, radar resolution and signal to noise ratio. These characteristics of the system define the accuracy, the precision and the capacity and quality of detection of the system.

3.3.1 Radar sensitivity

The radar sensitivity is defined by using the radar equation 2.11. in terms of the equivalent reflectivity factor $Z(r_o)_{min}$ as it is shown in equation 3.5, 3.6, and 3.7.

$$Z(r_o)_{min} = P_r \left(\frac{2}{c\tau} \right) \left(\frac{\lambda^2 4\pi^3}{P_t G_o^2} \right) \left(\frac{8\ln 2}{\pi\theta_1\phi_1} \right) \left(\frac{r_o^2}{\pi^5 |K|^2} \right) \quad (3.5)$$

$$Z(r_o)_{min} = DP_r \left(\frac{1}{\tau} \right) \left(\frac{\lambda^2}{P_t G_o^2} \right) \left(\frac{1}{\theta_1\phi_1} \right) (r_o^2) \quad (3.6)$$

Where D is a constant related with the medium and the target (in this case drops of water) and the received power can be related with the signal to noise ratio by $P_r = P_{MDS} SNR$, where P_{MDS} is the minimum detectable signal due to the thermal noise $P_{MDS} = KBTf_n$, where K is the Boltzman constant and, B corresponds to the bandwidth, T is the temperature in Kelvin and f_n is the noise figure, which in most of the cases aim to be less than $5dB$. The SNR is the minimum signal to noise ratio. Equation 3.6 can be expressed in dBZ as

$$Z(r_o)_{min}[dBZ] = P_{MDS}[dBm] + SNR[dB] + C[dB] + 20\log(r_o[km]) \quad (3.7)$$

From the equation 3.6 can be shown that the sensitivity of the radar is related to the pulse width of the transmitted waveform for longer pulses the sensitivity is better, which means that at certain r_o the value of Z_{min} is lower for longer pulses and so this allows a more efficient use of the average power capability of the radar.

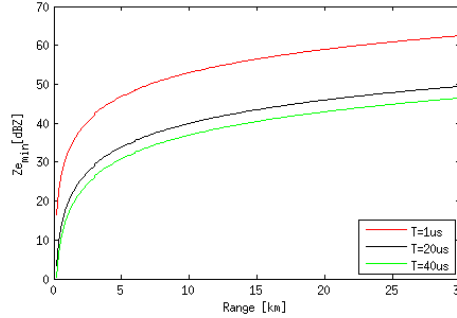


Figure 3.3: Radar Sensitivity

The curves shown in figure 3.3 correspond to the sensitivity evaluated with the specifications of the D3MON radar (tables 4.1 and 4.2) for K_u – band assuming that the target corresponds to rain and without using any compression.

When pulse compression is used the value of P_{MDS} changes, due to the change in the bandwidth, as well as the SNR value which depends on the transmitted waveform. Those changes generate improvement in matter of sensitivity which means that the values of the Z_{min} are smaller for all r .

Calibration is critical for evaluating sensitivity of the radar and depends on the type of waveform used in transmission[19]. In order to consider the calibration factor Z_o it is necessary to add this factor in the equation 3.7.

3.3.2 Radar Resolution

The radar resolution is related with the capability to distinguish between two or more different target which are close in range. As it was show in section 2.5

the resolution is related to the bandwidth of the compressed signal. Figure 3.4 presents the relationship between them, and it is evident that for bigger bandwidths the range resolution is small what means more capability of detection when the targets are near in range.

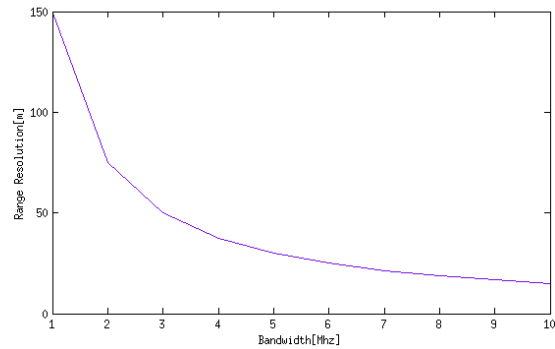


Figure 3.4: *Range resolution vs Bandwidth*

When the targets are sufficiently separated in range the detection of them is achievable with either unmodulated or modulated pulse, but when the targets are too close to each other the detection using the unmodulated pulse becomes unsuitable. Figure 3.5 illustrates the following situation: A single unmodulated pulse with pulse width $\tau = 20\mu s$ and a frequency modulated pulse with pulse width $\tau = 20\mu s$ and compression bandwidth $BW = 3.6MHz$ are generated as the transmitted pulse of the radar system. The output of the matched filter (MF)(see figure 3.2)is plotted in both cases in order to evaluated the results for both cases: when the targets are sufficiently separated and when are in the same range.

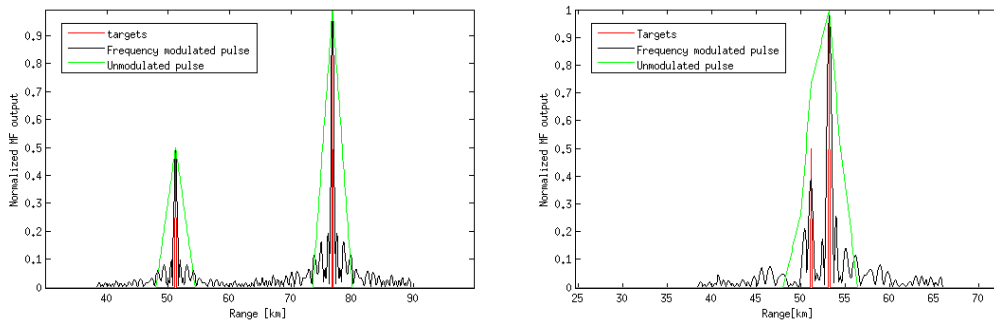


Figure 3.5: *Range resolution*

In the left figure the targets are separated $25.6km$ and as it is shown the detection of both targets is possible with and without modulation in the transmitted pulse. On contrary, in the right figure the targets are separated just $2km$ and the unmodulated pulse is not capable to detect the one of the targets this is due to the fact that for this case the range resolution is $3km$ and the system will not be able to detect any target within this range. In the other

case the range resolution is determined by the compression bandwidth and is $41.66m$ and allow the detection of the 2 targets.

In order to measure the range resolution Pebbles in [5] define the time resolution constant t_{res} as the width of a rectangular function equivalent to an ambiguity function cut in the sense that it has the same maximum amplitude and the same area (see Appendix B). Taking into account this definition a small T_{res} means good range resolution and then the use of wideband signals that must be treated carefully because of the presence of sidelobes can interfere in detection. For this reason the proposed interpretation is related with the separation between targets and then as the separation becomes greater than T_{res} the resolution is better.

3.3.3 Range sidelobes and weighting

In order to study the influence in SNR that the different signal processing techniques implemented within the radar system have there are two measures that are often used:

1. ISL-Integrated sidelobe level

Compares the total power contained within the sidelobes to the power contained within the main lobe. The ISL is given by the equation

$$ISL = 10\log \sum \frac{x_i^2}{x_o^2} \quad (3.8)$$

2. PSL-Peak sidelobe level

Compares the size of the highest sidelobe to the size of the main lobe. The PSL is defined as

$$PSL = 10\log \frac{\max(x_i)^2}{x_o^2} \quad (3.9)$$

In equations 3.8 and 3.9 , x_i is i -sidelobe power, x_o corresponds to the total mainlobe power.

3.4 Pulse compression system

The choice of the pulse compression system depends on the type of waveform selected and the method of generation and processing [18]. The big issue in implementing pulse compression is the presence of sidelobes which can cause false alarms in detection. In this section the idea is to look for different methods that allow to reduce this undesirable effect of the pulse compression. In the first part alternatives waveforms (non-linear modulation and complementary codes) are compared with the traditional and more often used waveforms (Linear modulation and barker codes), then some mismatched techniques applied to the output of the matched filter for traditional waveforms are compared and finally all the results are put together in order to propose a suitable and realisable solution for D3MON radar system.

A big disadvantage of pulse compression implementation is the presence of range sidelobes which causes modification in the returns in range overall in dispersed targets as it is the case of meteorological phenomenon that are the

point of interest of weather radars. For this reason sidelobe suppression become critical for this type of applications and it is made by either tapering the matched filter response or weighting the transmitted pulse or both. This can be done in frequency domain as well as in time domain [8]. This implementation is known as *Mismatching*.

3.4.1 Reducing sidelobes

In current radar applications one of the most common techniques applied in pulse compression is to use a classical LFM or binary phase code waveform and to add a weighting filter at the output of the matched filter as in figure 3.6 this configuration allows to obtain acceptable side lobes. Another way to do this is by applying the weighting directly to the transmitted waveform before going through the matched filter.

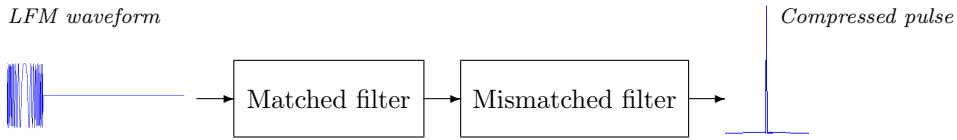


Figure 3.6: Pulse compression system using LFM

The mismatched can be done by using different types of filters which, because of their specific characteristics, will affect in different ways the peak side lobe, the integrated side lobe and the mismatch loss of the compressed pulse. The easiest way to implement the mismatched technique is by applying a window in the transmitted pulse and this technique is going to be evaluated in the following section.

Windowing

Windowing is a technique which uses time domain weighting functions looking for reduction in the oscillations by limiting a Fourier series. The time domain weighting functions or windows are non-negative functions whose shape varies depending on which characteristics of the signal are desired.

In order to evaluate this technique 4 different windows were chosen:

+ Hamming window

$$w(n) = 0.54 - 0.46 \cos\left(\frac{2\pi n}{N}\right) \quad 0 \leq n \leq N \quad (3.10)$$

+ Hanning window

$$w(n) = 0.5 \left[1 - \cos\left(\frac{2\pi n}{N}\right) \right] \quad 0 \leq n \leq N \quad (3.11)$$

+ Kaiser window

$$w(n) = \frac{I_0\left(\pi\alpha\sqrt{1 - \left(\frac{2n}{N-1} - 1\right)^2}\right)}{I_0\pi\alpha} \quad (3.12)$$

Where I_0 are the zero order modified Bessel function of the first kind.

+ Chebyshev window [27]

$$w(n) = \frac{1}{N} \left[1 + 2r + \sum_{m=1}^M T_{2M} \left(x_0 \cos \left(\frac{2\pi n}{2M} \cos(m\theta_n) \right) \right) \right] \quad (3.13)$$

T_m are the Chebyshev polynomials, r is the range, $x_0 > 1$, $n = 2M + 1$ and $-M \leq n \leq M$.

This windows were applied to the linear frequency modulated transmitted waveform, and the results are shown in figure 3.7

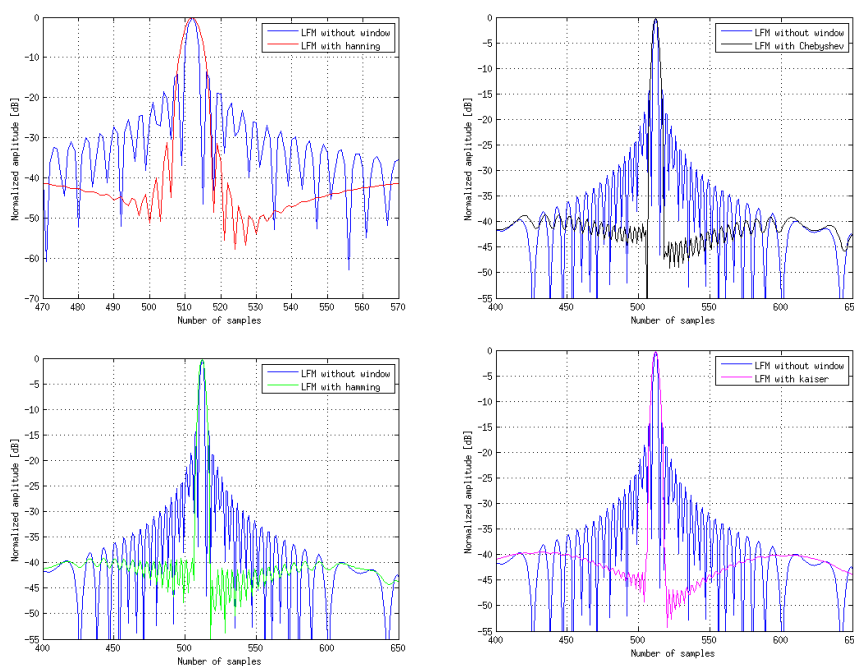


Figure 3.7: *Windowing*

As It can be appreciated from the figure all the chosen windows contribute to our goal: reduction of side lobes, but there is a damage in other characteristics of the desired signal: less resolution and mismatch losses are generated. The hanning window is not convenient for the system because the width of the main lobe is too large and the side lobes are reduced to $-31.28dB$. The other three windows have higher performance in both aspects all three have the peak side lobe around $-40dB$ between the three the one that provides more resolution is the Chebyshev window.

3.4.2 Transmitted signal design

Pulse compression using Complementary codes

Complementary codes are defined as a pair of sequences with the same length that follow the following property: for any given separation the number of likes

and unlikes between the elements of each sequence is equal for both sequences. This characteristic means symmetry and yield to the attractive aspect of using complementary codes which is the fact that the periodic autocorrelation function is zero everywhere expect at the zero shift. Thus by using this kind of codes in the transmitted waveform in the system a reduction in the sidelobes can be achieved.

One of the most well known complementary codes are the Golay codes. Table 3.1 shows some Golay codes taken from [28].

Length	A	A'
2	+1 +1 +1 +1	-1 +1 +1 -1
4	+1 -1 +1 +1 +1 +1 -1 +1	-1 +1 +1 +1 +1 +1 +1 -1
8	+1 -1 +1 +1 -1 +1 +1 +1 +1 +1 +1 -1 +1 +1 -1 +1	-1 +1 -1 -1 -1 +1 +1 +1 +1 +1 +1 -1 -1 -1 +1 -1
16	-1 -1 +1 -1 +1 +1 +1 -1 +1 -1 -1 -1 -1 +1 -1 -1 -1 -1 +1 -1 -1 -1 -1 +1 -1 +1 +1 +1 -1 +1 -1 -1	+1 +1 -1 +1 -1 -1 -1 +1 +1 -1 -1 -1 -1 +1 -1 -1 -1 -1 +1 -1 -1 -1 -1 +1 +1 -1 -1 -1 -1 +1 -1 +1

Table 3.1: Golay codes

In order to use this codes in the radar system the compression block will be modified as in figure 3.8.

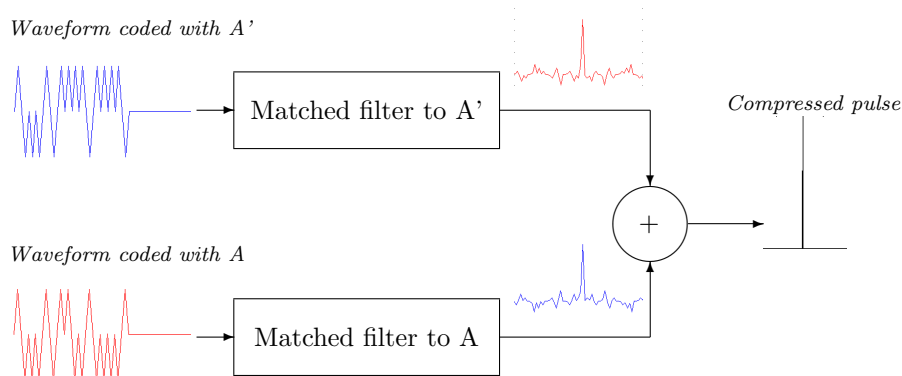


Figure 3.8: Pulse compression system using LFM

The idea then is to generate 2 different transmitted signals coded with the pair of codes and pass them through their corresponding matched filter. The compressed pulses generated in the output of each matched filter are summed in order to take advantage of the property of their autocorrelation function and in this way the total compressed pulse will be a function without sidelobes. The value of the peak at the output corresponds to twice the length N of the code that is being used.

Figure 3.9 illustrates the compressed pulse by applying Golay codes and comparing it with the compressed pulse obtained with a waveform that uses barker codes.

As it is shown the PSL for the barker codes is equal to -22.2789 whereas that by using Golay codes the PSL value is around $-212.6dB$. In principle this

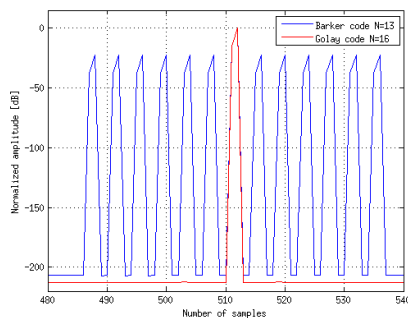


Figure 3.9: *Compressed pulse using barker and Golay codes*

waveform could solve the problem, but in practice is difficult to implement due to the fact that 2 signals have to be generated and transmitted and then the interaction with the target will affect the properties of the signal this implies that the cancellation due to the sum between both compressed pulses will be hardly achieved.

Pulse compression using Non linear modulation (NLM)

By using a non-linear frequency modulated waveform the improvements in matter of power conservation and sidelobe suppression are enhanced. There is no need of additional weighting in order to reduce the sidelobe because the waveform is designed to have some specific characteristics in the spectrum looking for eliminate the losses caused by the mismatched technique.

There are two well known types of non-linear frequency modulated waveforms: Symmetrical and asymmetrical. A symmetrical waveform is a even function in the frequency vs time plane and a asymmetrical waveform is a pair function in the same plane. It is important to note that a non linear FM waveform that is asymmetrical retains some characteristics of the LFM modulated waveforms.

Generation of non linear FM modulated signals

The task of generate non linear FM modulated (NLFM)signals involves the design of the amplitude $a(t)$ and frequency $\theta(t)$ modulations in equation 2.1 looking for modify the shape of the spectrum which avoids energy losses [20] and saphing the spectrum includes also modifying the form of the time response.

The transmitted signal $s(t)$ can be written as

$$s(t) = a(t)e^{j\phi(t)} \quad (3.14)$$

where $\phi(t)$ is the phase of signal which includes the frequency modulation. The spectrum of the signal of the transmitted signal $S(\omega)$ is given by its Fourier transformation and defined by its magnitude $U(\omega)$ and phase $\theta(\omega)$. The expression of $S(\omega)$ is complex to solve when a NLFM is used. For this reason putting $a(t)$ to vary slowly in relation with the phase $\phi(t)$ a good approximation can be done using the stationary phase principle.

The principle of the stationary phase establishes that the major contribution to the spectrum $S(\omega)$ at any frequency ω is made by that part of the signal which has instantaneous frequency $\omega_i(t)$ [21]. In mathematical terms is

$$\frac{d}{d\omega}[\theta(\omega) - \omega t] = 0 \quad (3.15)$$

The magnitude square of the transmitted signal is equal to $|u(t)|^2 = |U(\omega)|^2 \frac{2\pi}{\theta''(\omega)}$

From the equation 3.15 it is clear that $\theta''(\omega) = \frac{dt}{d\omega}$ and so the magnitude square of the transmitted signal $|u(t)|^2$ will be equal to the magnitude square of the spectrum $|U(\omega)|^2$. By integrating $|u(t)|^2$ from $-\infty$ to $+\infty$ this equality would yield to the Parseval theorem but in order to obtain the time group delay t the integral 3.16 is formed.

$$\int_{-t}^t |u(\tau)|^2 d\tau = \int_{-f}^f |U(\omega(\varepsilon))|^2 d\varepsilon \quad (3.16)$$

In this specific case looking for good efficiency in the system which uses solid state transmitters a square pulse is used. This implies constant power such that $u(t)^2 = \frac{1}{\tau}$ in the interval $\frac{-\tau}{2} \leq t \leq \frac{\tau}{2}$ so equation 3.16 becomes

$$t = \frac{\tau}{2} \int_{-f}^f |U(\omega(\varepsilon))|^2 d\varepsilon \quad (3.17)$$

Solving 3.17 for $t(\omega)$ the information about the time group delay is provided. As $t(\omega)$ is equivalent to the inverse of the instantaneous frequency in time[22], then by inverting $t(\omega)$ the instantaneous frequency $w_i(t)$ is obtained.

The phase $\phi(t)$ in 3.14 is given by

$$\phi(t) = \int_0^t w_i(\tau) d\tau \quad (3.18)$$

The design procedure is summarized in figure 3.10

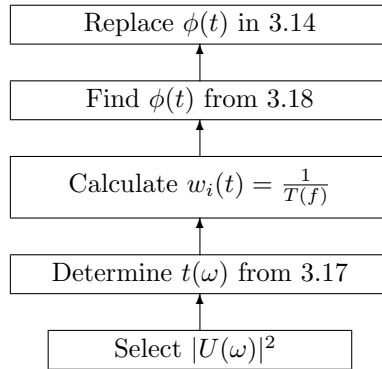


Figure 3.10: *NLFM waveform design*

Under this design procedure different NLFM waveforms can be generated. The idea then is to study them in order to determine which one of these can provide good performance for the system under study. In this part 5 different shapes of the spectrum are evaluated:

- Power- n cosine spectrum [23]

The spectrum function is given by 3.19

$$|U(w)|^2 = \left[\cos \left(\frac{\pi(f_o - f)}{B} \right) \right]^n \quad (3.19)$$

Figure 3.11 shows the frequency vs time characteristic for different values of n and the matched filter output for each case.

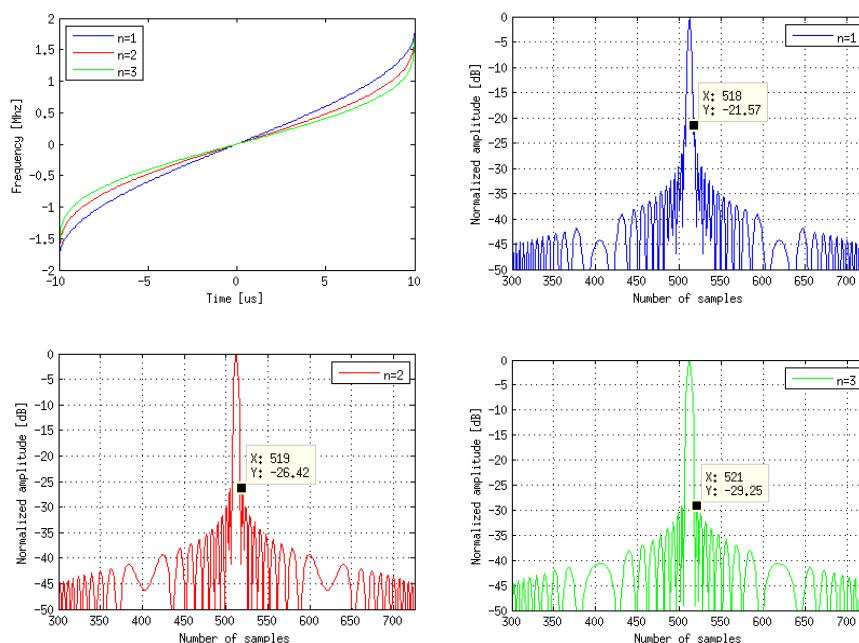


Figure 3.11: *Power- n cosine spectrum*

As it is shown in the frequency vs time curve by increasing the value of n the slope in the central part of the curve is smaller and in the edges the frequency changes more quickly. At the output of the matched filter we can observe that this fact causes better values of PSL and some additional losses in resolution.

- Cosine-squared on pedestal spectrum [23]

The spectrum function is given by 3.20

$$|U(w)|^2 = k + (1 - k) \left[\cos \left(\frac{\pi f}{B} \right) \right]^2 \quad (3.20)$$

The compression system was evaluated with this spectrum for different values of k . Table 3.2 depicts the results obtained.

- Taylor weighting spectrum [18]

k	PSL [dB]
0.088	-28.95
0.18	-33,06
0.34	-30.7
0.5	-25.8

Table 3.2: PSL values for cosine-squared on pedestal spectrum

The spectrum function is given by 3.21

$$|U(w)|^2 = 1 + \sum_{m=1}^{\bar{n}-1} f_m \cos\left(\frac{2\pi f m}{B}\right) \quad (3.21)$$

where f_m correspond to the Taylor coefficients¹. By using this spectrum a PSL of -32.16dB is reached.

- Tangent based waveform

The instantaneous frequency is given by 3.22

$$f(t) = \frac{B \tan\left(2\beta \frac{t}{B}\right)}{2 \tan(\beta)} \quad (3.22)$$

Where $\beta = a \tan(\alpha)$. Depending on the value of alpha the behaviour of the matched filter output varies. Table 3.3 shows the value of PSL for different α .

α	PSL [dB]
2	-25.14
1	-18.01
0.9	-17.73
0.7	-16.5
0.5	-15.68
0.1	-13.93

Table 3.3: PSL values for tangent based waveform

- Zac transform based waveform

This is an approach which uses the Zac transform² as the starting point of the NLM waveform design and is implemented by C. Leśnik in [29]. According to the reference the instantaneous frequency is given by 3.23

$$\omega_i(t) = \frac{t - \frac{\tau}{2}}{\sqrt{k^2 - \left(t - \frac{\tau}{2}\right)^2}} \quad (3.23)$$

where $k = \left(\frac{\tau}{2}\right)^2 \frac{w^2 + c}{w^2}$.

¹Appendix B shows the method to calculate them

²see appendix C

Replacing k in equation 3.23 and evaluating it in $t = 0$ and $t = \tau$ the expression for the bandwidth B can be written as

$$B = \frac{2w}{\sqrt{c}} \quad (3.24)$$

In principle w is set equal to B so the value of c is 4. In any case the value of c can be modified in order to obtain certain characteristics in the signal, but it will affect the bandwidth characteristics of the signal.

By following equation 3.18 the phase information is obtained. The frequency and phase characteristics for this waveform are depicted in figure 3.12

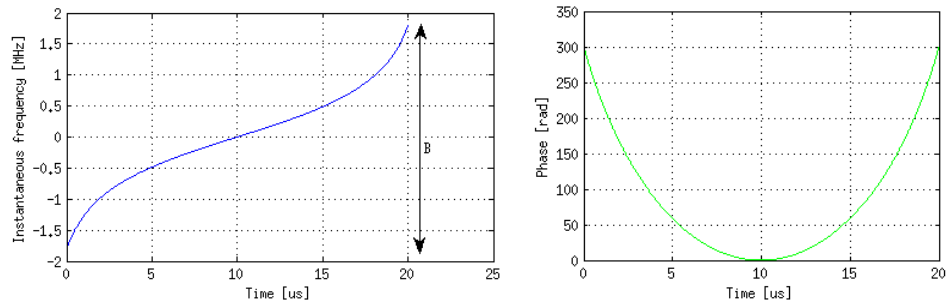


Figure 3.12: Frequency and phase characteristics of Zacc transform based waveform

After the matched filter the compressed pulse is as in the left part of figure 3.13. As it is shown the sidelobe level is around $-34.93dB$. The right part of this figure shows the effect over the compressed pulse when a Kaiser window weighting is applied to the transmitted Zacc transform based waveform. The improvement in matter of PSL is of $-50dB$ in comparison with the pulse without weighting, so the sidelobe level is around $-85.99dB$.

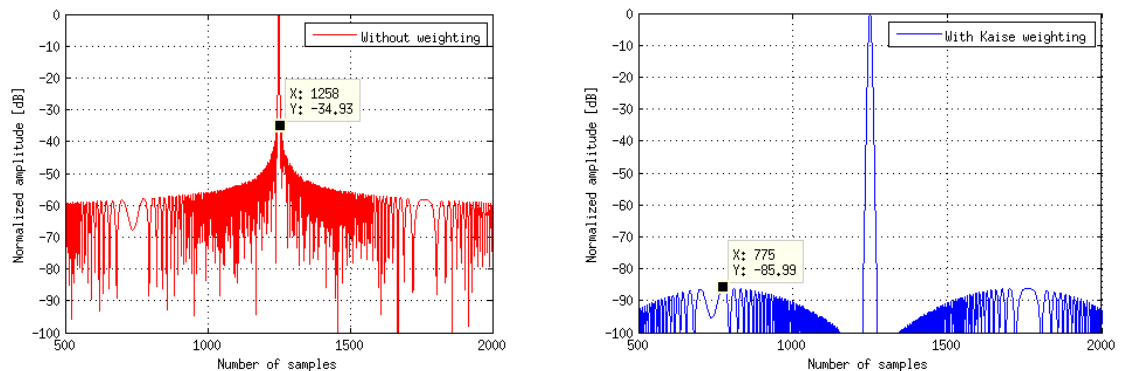


Figure 3.13: Matched filter output for Zacc transform based waveform with and without weighting

Remarks

* LFM vs NLM

The LFM waveform is well known as one of the easiest waveforms to generate and because of this it has been widely used. One of the major disadvantages of LFM waveform is that the use of the weighting is usually need in order to reduce the time sidelobes of the compressed pulse. The use of the this weighting causes in most of the cases losses in SNR. In the other hand the use of NLM waveform hasn't been a common solution for compression even though it has several advantages. The low level of the sidelobes reached possible without no weighting is perhaps the most attractive characteristics given by using this type of waveform. The sidelobe level depends on the waveform design and it used is compatible with the matched filter approach.

In terms of performance, by using LFM without weighting the value of sidelobes is about $-13.85dB$ with notable losses in terms of resolution. The use of polynomial NLM without weighting provides sidelobe level of $-34.93dB$ with a lot better resolution than the previous case. However the mismatched technique become necessary in both cases. By applying weighting the output of the matched filter using LFM waveform exhibits sidelobes of $-40dB$ in the best case with notable losses in resolution. In the other hand when the transmitted signal is a NLM waveform the compressed pulse has sidelobe value of $-85.99dB$ with higher resolution.

* Barker codes vs Complementary

Binary codes in general provide the good range sidelobes depending directly on the length of the code N and the code itself. By using Barker code $N = 13$ the PSL reached is around $-22.3dB$ whereas using Golay code $N = 16$ the PSL after compression is about $-212dB$. In the case of complementary codes the peak amplitude at the output of the matched filter is twice the length of the code while for the barker code is equivalent to the length of the code, so apparently the complementary codes give better performance in theory but in practice to reach the desired phase in the two signals that are needed will be a problem, because of the presence of the phase noise added by the system.

* Phase modulation vs Frequency modulation

The use of phase coded waveform has become attractive because of its easy generation. By using phase modulation in the transmitted waveform a fine resolution can be obtained. One of the disadvantages of the use of phase modulation is the presence of the phase noise in the system (transmitter and receiver), which in the practice affects the properties of the desired phase coded signal making it less efficient for the system. Depending on which kind of waveform is chosen in either phase or frequency modulation the use of an additional weighting is determined by the waveform design. In the other hand the frequency modulation even more attractive in the sense that it has been used in a lot of radar implementations and a good performance in terms of resolution, sensitivity and signal to noise ratio has been achieved with less losses caused by the phase noise in the system.

Chapter 4

The high frequency radar (D3MON)

4.1 Generalities

The main goal of this project is to contribute in the development of a cheap high frequency radar ($16 - 90GHz$) with high operational confidence with measurement capabilities that satisfies the needs in specific areas which include: monitoring of meso-scale phenomena and non- meteorological targets for the air traffic, defense sector and traffic safety safety in general. The information is expected to be used for icing, high resolution wind fields, clouds and precipitation. High frequency radar technology is also important for the study of cloud droplet processes in climate and weather processes research, and also for the development of climate and numerical weather prediction (NWP) models.

The current limitations for the operational use high frequency radars include the expensive and unreliable hardware technology. The new radar technology to be used in this system includes to work with solid state components. This would significantly decrease the component costs of a radar system, and simultaneously increase the instrument reliability. In order to reach this objective The possible signal processing techniques would include the traditional FM-CW and the appliance of digital stepped frequency/pseudo noise modulation.

4.1.1 Radar specifications

In order to fulfill the purpose of this project it is important to take into account the general specifications of the system as well as the specific requirements in the transmitter and receiver where the signal processing takes place.

System specifications

The general specifications of the system were well-established and are presented in table 4.1. In some of the requirements there are constraints related with cost and other performances for instance the minimum detectable signal and the maximum unambiguous doppler velocity (in Ka and W bands).

Parameter	Requirement
Center Frequency	Ku-Band $13.96GHz \pm 25MHz$ Ka-Band $33.5GHz \pm 25MHz$ W-Band $95.1GHz \pm 25MHz$
Frequency Bandwidth	For all Frequencies $10MHz$
Range Resolution	Minimum range resolution $30m$
Pulse Length	For all frequencies from $0,1\mu s - 1\mu s$ Maximum duty cycle 30%
Pulse Repetition time	For all Frequencies $0,3\mu s - 1\mu s$
Minimum operational range	$150m$
Minimum detectable signal	$-30dBz@1Km$ and range resolution $150m$
Maximum unambiguos doppler velocity	$10 \frac{m}{s}$
Maximum range	$30Km$
Angular Coverage	Azimuth: $0 - 360^\circ$ Elevation: $-0,2 - 90,1^\circ$
Antenna pointing accuracy and repeatability uncertainty	less than $0,2^\circ$

Table 4.1: D3MON specifications

Figure 4.1 shows the general high level block diagram of the D3MON high frequency radar.

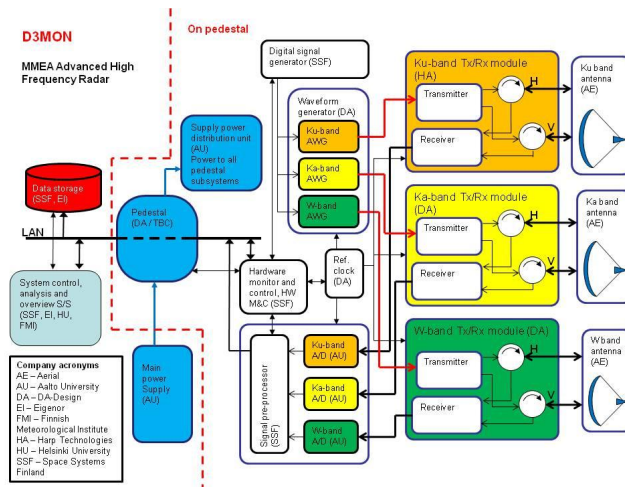


Figure 4.1: D3MON general block diagram

Transmitter and receiver specifications

Table 4.2 summarize the requirements for the transmitter and receiver module of the D3MON radar.

Parameter	Requirement
Transmitter type	Solid state amplifiers
Peak power	Ku-Band 60W Ka-Band 20W W-Band 0,5W
Duty Cycle	30%
Phase Noise	Better than $0,2^\circ$
Phase Linearity	$\pm 1,5^\circ$ over $2B_{Tx}$
Gain Flatness	$\pm 1,5dB$ over $2B_{Tx}$
Dynamic Range	For all Frequencies 90dB
Noise figure	Better than 5dB
Analogue IF output range	within 5 – 120MHz

Table 4.2: Transmitter and receiver specifications

4.2 Range resolution

In order to achieve the requirement of minimum operational range of 150m It is necessary then to use a pulse with $\tau = 1\mu s$, but using a pulse with this characteristic means to decrease the duty cycle $d = \frac{\tau}{PRT}$ which causes losses in terms of detection due to the direct relation between them $P_{rav} = P_t d$ in the case of a pulsed radar[17]. In addition to this the use of solid state amplifiers will keep decreasing the value of P_{rav} because this technology exhibits low peak transmitted power. However the detection can be improved by increasing the pulse width.

Then the question is how to have both characteristics in a unique waveform. The first approach considered was to modulate the transmitted waveform taking advantages of the pulse compression. In this way the system counts with the properties of using a large pulse without losing resolution.

4.3 Frequency diversity principle

The blind zone phenomena is caused when the pulse width is increased. It occurs due to the fact that while a long pulse is being transmitted the echos from the targets that are close to the radar can't be detected because the antenna is being used for transmission. In order to cover this blind zone a short pulse is needed. In any case the use of this approach causes losses in sensitivity but it can be managed by making a combination of pulses with different pulse widths and the sensitivity will vary as it is shown in figure 4.2.

It is important to highlight that the design of each pulse will affect the sensitivity characteristics of the system. As it was mentioned in section 3.3.1 the use of pulse compression and the design of the waveform will affect the value of P_{MDS} and SNR . For this reason each one of the pulses must be designed so that they comply with the requirements in matter of range resolution and sensitivity.

The use of this approximation implies to put all the sub-pulses in one single pulse. All the sub-pulses have to be orthogonal in time and frequency so that the final waveform describes a frequency diversity wideband signal.

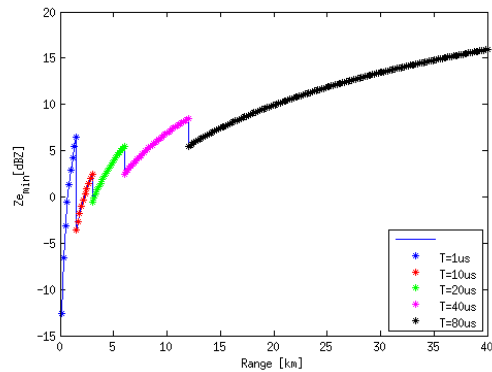


Figure 4.2: *Minimum reflectivity caused by the use of combination of pulses*

Figure 4.3 depicts the envelope of the transmitted pulse using 3 pulses of $1\mu s$, $20\mu s$ and $40\mu s$.

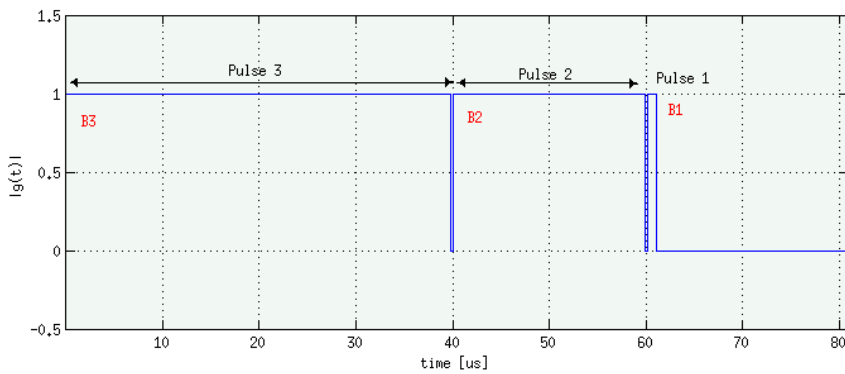


Figure 4.3: *Complex envelope of transmitted pulse with sub-pulses*

Other important fact is that the use of more than one pulse can cause distortion effects which can be reduced getting the corresponding information of each pulse. This can be solved by separating the pulses in frequency so that the receiver will be able recognize each component.

4.4 The best choice

Taking into account the features exposed until this point the compression system for the D3MON radar will be built up with a transmitted pulse with certain number of sub-pulses. Each one of these pulses has some specific characteristics of length, frequency modulation, bandwidth and carrier frequency.

The simulated radar signal is convolved with each sub-pulse and these results are sent to the compression filter. The compression filter is a set of filters. The number of filters depends on the number of sub-pulses. The most important characteristic of these filters is that each one of them has to be matched to a

specific sub-pulse. In this way the compressed pulse is the sum of the compressed pulse at the output of each filter. Supposing a waveform consisting of 2 sub-pulses figure 4.4 illustrates the situation.

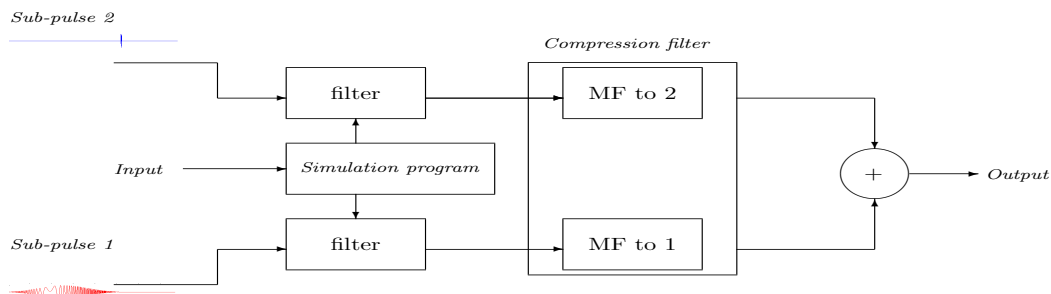


Figure 4.4: Simulation scheme when transmitted waveform is a set of sub-pulses

In this section there will be evaluated different configuration of the waveform: varying number of sub-pulses, changing the values of the bandwidth of each sub-pulse and the type of modulation of each pulse. This in order to determine which configuration provides the better performance in *PSL*, *ISL*, resolution and sensitivity.

The evaluation was done supposing an input profile consisting of a $50dB$ spout at $15Km$ and minimum constant value for all the other ranges.

4.4.1 Deciding number of pulses

As it was shown previously the idea is to build the transmitted waveform with sub-pulses, but it means the use of additional filters. So the idea is to design the waveform as simpler as possible getting the best performance. Because of this our interest is focused in the transmitted waveform consisting of either 2 or 3 pulses.

The lengths of the pulses for 2 pulses case are: $\tau_1 = 40\mu s$ and $\tau_2 = 1\mu s$. For 3 pulses case the lengths are: $\tau_1 = 40\mu s$, $\tau_2 = 20\mu s$, $\tau_3 = 1\mu s$. For the bigger pulses Zac based waveform was used. Both were weighting using a kaiser window with sidelobe attenuation parameter of 6.

Table 4.3 presents the results obtained for transmitted waveforms with different bandwidths BW for both cases 2 and 3 pulses. In the 3 pulses case the bandwidth for the 2nd and 3rd pulse are equal.

BW	Np	B1	B2		PSL	ISL	Res
5Mhz	2	1Mhz	4Mhz		-83.75dB	-37.04dB	37.5m
	3		2Mhz	2Mhz	-75.03dB	-21.79dB	75m
10Mhz	2	1Mhz	9Mhz		-81.95dB	-40.50dB	16.67m
	3		4.5Mhz	4.5Mhz	-78dB	-32.22dB	33.33m
20Mhz	2	1Mhz	19Mhz		-66.06dB	-40.97dB	7.89m
	3		9.5Mhz	9.5Mhz	-64.89dB	-34.92dB	15.79m

Table 4.3: *PSL* and *ISL* values for compressed pulse using 2 and 3 pulses in the transmitted waveform

In either case it is evident that by increasing the values of BW the ISL is better while the value of PSL becomes bigger. In matter of resolution the use of 2 pulses assures lower values in comparison with the resolution obtained when 3 pulses are used. Once again by increasing the BW the the preformance in resolution is better. For all the considered bandwidths there is a common behaviour with regard to the PSL and the ISL. When 3 pulses are used the value of PSL is greater and the ISL is smaller. This means that apparently the use of 2 pulses with small bandwidth BW will responds better to our needs highlighting the fact that regarding the specifications of the system the solution for $5Mhz$ and $10Mhz$ with 2 or 3 pulses are within the requirements of PSL and ISL.

However it is important also to evaluate the sensitivity for both cases. Figure 4.5 depicts the curve of sensitivity for all the both cases with different values of BW.

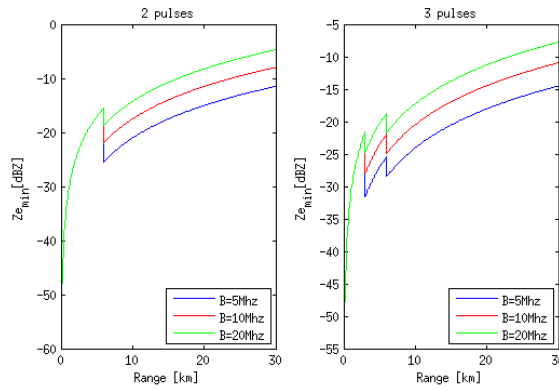


Figure 4.5: Sensitivity curve for a waveform built up with 2 and 3 pulses

In this figure one can appreciate that increasing the bandwidth BW of the transmitted waveform decreases the sensitivity of the system. So using low values of BW is again good for the system. Comparing the behaviour of the curves with lower BW for 2 and 3 pulses it is evident that by using 3 pulses the values over all the range are smaller and the curve is smoother than when 2 pulses are used. Looking at the curves for 3 pulses with $5Mhz$ and $10Mhz$ it is important to mention that the curve for $10Mhz$ presents a steady behaviour along the range.

Taking into account these results one can deduce that the solution consisting in a waveform made by 3 pulses with $10Mhz$ of Bandwidth fulfills better the requirements in matter of sensitivity, PSL, ISL and resolution than the other options.

4.4.2 Changing the values of Bandwidth for each pulse

Now considering the solution with 3 pulses and BW of $10Mhz$, the idea is to find the better combination of bandwidths for the pulses. Table 4.4 presents the results obtained for different configurations of the transmitted waveform.

Total Bandwidth	B1	B2	B3	PSL	ISL	Res
10Mhz	1Mhz	4Mhz	5Mhz	-78.21dB	-32.22dB	30m
		5Mhz	4Mhz	-79.85dB	-31.92dB	30m
		6Mhz	3Mhz	-78.18dB	-27.09dB	25m
		3Mhz	6Mhz	-77.64dB	-30.17dB	25m

Table 4.4: PSL for compressed pulse 3 pulses in the transmitted waveform changing the bandwidth of the pulses

From this table one can conclude that for smaller values in B2 compared to B3 the performance in ISL is enhanced and the PSL is greater. The resolution is the same for those configurations with the inversed values of B2 and B3. Comparing the cases where $B2 < B3$ when B2 is greater there is an improvement in PSL and ISL, but here again the resolution is bigger. In the case of study the resolution given by the combination $B2 = 4Mhz$ and $B3 = 5Mhz$ is enough. Nonetheless the sensitivity has to be evaluated. Figure 4.6 depicts the sensitivity curve for the cases where $B2 < B3$ and $B2 = B3$.

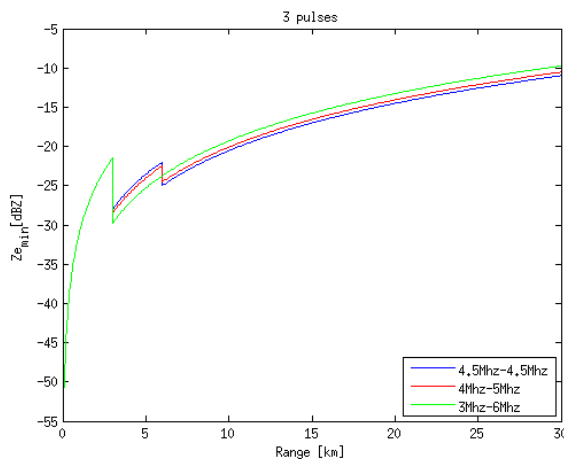


Figure 4.6: Sensitivity curve changing values of B2

As before one can highlight the fact that for both cases $B2 = 4Mhz$, $B3 = 5Mhz$ and $B2 = B3$ the sensitivity curve is smoother than in the case $B2 = 3Mhz$, $B3 = 6Mhz$. For this reason the choice is restricted to the cases where $B2 = 4Mhz$, $B3 = 5Mhz$ and $B2 = B3$. The final decision rests with the resolution requirement which is fulfilled by the waveform made up by the pulses with bandwidths of $B2 = 4Mhz$ and $B3 = 5Mhz$.

4.5 Proposed pulse compression system

Taking into account all the features and the simulations that were done. The most suitable compression system, which is going to be used in the 3 bands K_a , K_u and W , consists in:

- Waveform: Transmitted waveform with 30% of duty cycle, consisting of 3

sub-pulses. The sub-pulses lengths are $\tau_1 = 1\mu s$, $\tau_2 = 20\mu s$ and $\tau_3 = 40\mu s$ as it is shown in figure 4.7. Each sub-pulse is weighted with a kaiser window with sidelobe attenuation parameter of 6.

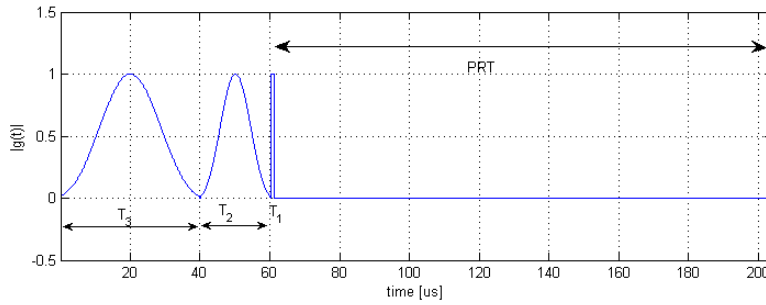


Figure 4.7: *Transmitted pulse envelope*

The ambiguity function of the proposed waveform is illustrated in figure 4.8. It is easy to see that the properties of this function give to our system good resolution in range and doppler.

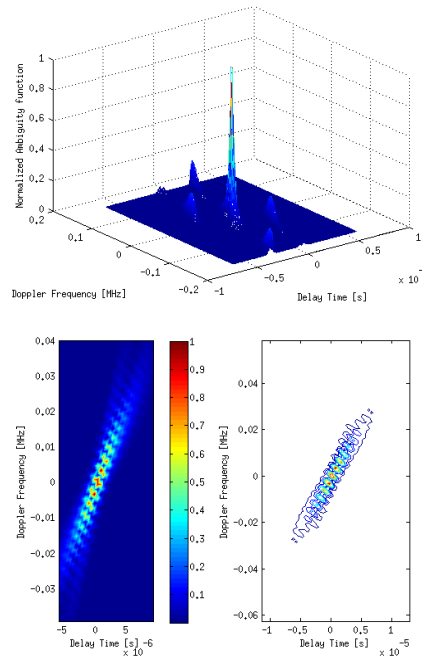


Figure 4.8: *Transmitted pulse ambiguity function*

The frequency characteristic for the transmitted pulse is presented in figure 4.9. As it is shown there it is evident that the 3 sub-pulses are orthogonal in frequency and in time. The carrier frequencies for the sub-pulses are respectively $f_1 = 20MHz$, $f_2 = 70MHz$ and $f_4 = 140MHz$.

Taking into account the previous study about the bandwidth of the sub-pulses the values of the bandwidths are set respectively to $B_1 = 1e6$, $B_2 = 4Mhz$ and $B_3 = 5Mhz$.

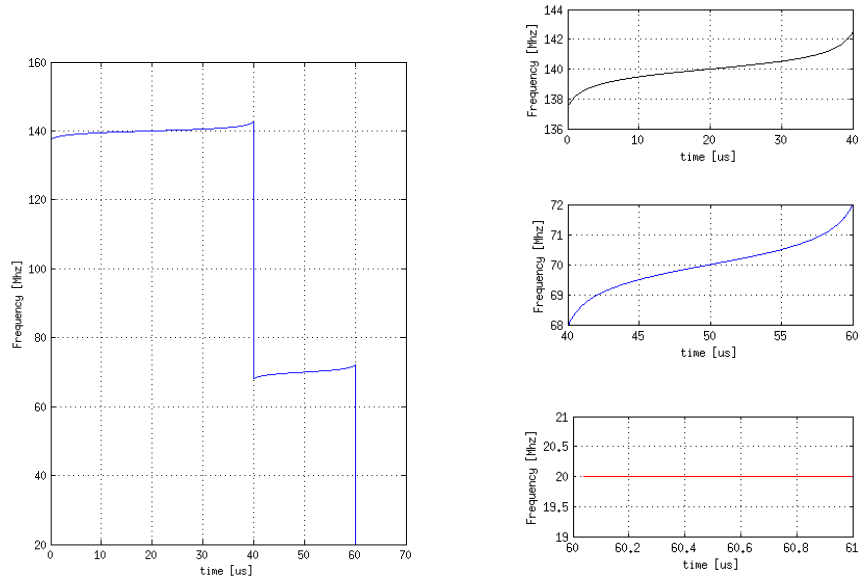


Figure 4.9: Frequency characteristic of the transmitted pulse

- Compression filter: The compression filter is the set of 3 matched filters. Each one of these filters corresponds to the optimum filter which maximizes the SNR ratio for each sub-pulses. The compressed pulse for the received signal is the sum of the outputs of the matched filters. Figure 4.10 shows the proposed set of filters.

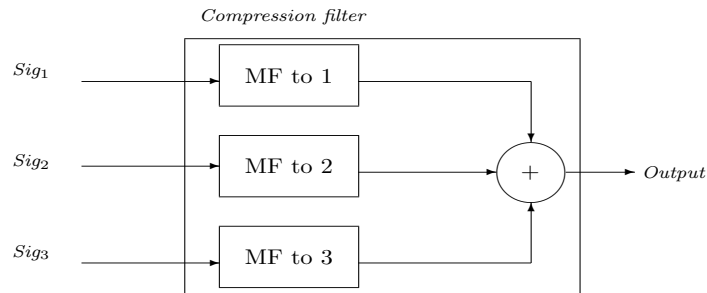


Figure 4.10: Simulation scheme when transmitted waveform is a set of sub-pulses

It is important to evaluate how much influence has each one of these filter over the others. In order to do so the frequency response is plotted in figure 4.11. From this picture it is evident that the filters are well separated in frequency. When the magnitude of one of them reaches its maximum, the magnitude for the others has lower values.

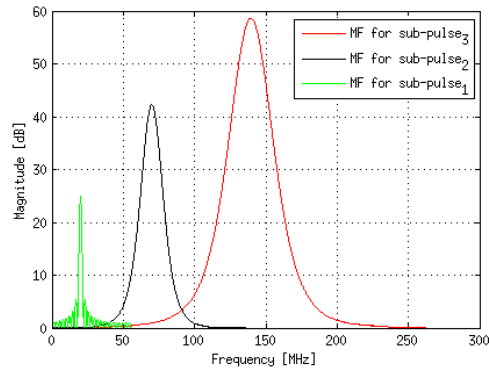


Figure 4.11: Matched filters frequency response

4.5.1 Evaluation

In order to evaluate how the proposed system works a simple input profile was chosen. The input consists in a triangular profile along 30Km . Its maximum occurs in 15Km , and the magnitude at this point is 40dB .

The simulation was done following closely the scheme in figure 3.2 and integrating the variation in the compression filter due to the specific characteristics of the proposed waveform.

The output of the system using the proposed compression system is depicted in figure 4.12.

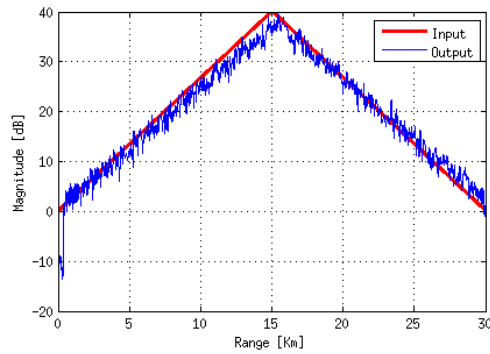


Figure 4.12: Input and output profile using the proposed compression system

Chapter 5

Discussion and recommendations

5.1 Conclusions

Pulse compression is a technique which allows to have high resolution weather radar measurements and high signal to noise ratio. In any case it is important to evaluate the performance of any compression technique. It was shown that by evaluating sensitivity, resolution, ISL and PSL a good approximation of the behaviour of the system can be done.

The use of a matched filter as the compression filter generates sidelobes in the compressed pulse. However this effect depends on the type of modulation used in the transmitted waveform. If the transmitted waveform has an autocorrelation function that exhibits low sidelobes then the compressed pulse obtained by using the matched filter will have an acceptable sidelobe level for meteorological applications.

Based on the study done in designing the ideal transmitted waveform one can conclude that the use of non-linear modulation waveforms provides by itself better performance in comparison with the traditional linear modulation technique. Nevertheless in either case the weighting of the transmitted waveform gives better performance in terms of PSL affecting in different proportions the resolution of the compressed pulse: for linear modulation the losses in resolution are higher, which becomes evident by looking at the width of the mainlobe.

Within the non-linear frequency modulated waveform studied the Zc transform based waveform provides the best performance in PSL and with additional weighting gives to the system good resolution and PSL lower than -80dB.

The use of long pulses makes necessary the use of more than one pulse in the transmitted waveform. This is due to the fact that while the radar is transmitting reception process is impossible creating a blind zone. However the use of more than one pulse causes losses in sensitivity and makes the system complex. For this reason the solution has to aim to simplicity, referring a number of pulses, and better sensitivity, which is achieved by choosing the appropriated length of each one of the sub-pulses. When more than one pulse is used in the transmitted waveform it is important to assure that those pulses are orthogonal in time and frequency.

5.2 Future work

The D3MON radar system is at this moment starting the 2nd year, so until this point the system specification and the preliminary design are done. For the next 4 years the schedule is fixed and the idea is to start with the design and testing procedure through simulations in order to bear out the results obtained in the first phase. The following step will be the manufacturing, testing and integration ending with the demonstration of different applications.

Following the investigations described in this project, a number of subject for research could be taken up, involving the pulse compression system proposed:

- By proposing a new non linear waveform for the transmitted pulse look for the way to eliminate the weighting part and obtain at least the performance reached with the couple weighting-waveform.
- How to take advantage of the phase-modulated waveforms knowing that the presence of phase noise in transmission and reception could affect the performance of the system.
- A complete study could be done about the advantages of using the proposed pulse compression system in for instance: Microwave interaction with precipitation and cloud droplets, high resolution precipitation estimation, microphysical precipitation research, air traffic safety (icing conditions, wake vortices), bird detection, climate change, safety and military applications, etc.

5.3 Critical analysis of the research

Developping this project at Helsinki University was the first experience I had working for a research institution. The initial expectations were really high: to work in a foreign country, to get to share time with people that have been in the field for some time, to arrive with the basic concepts about the subject. Those were things that before starting this experience I was worried about, but then they just became one more challenge in my professional life.

This experience was an amazing and complete learning process. It started with the information search about the subject and the establishment of my own work methodology. This took me some time, but thanks to the guidance of my supervisor I could go through the process without any pressure and getting more and more involve on it. The program I used to perform the simulations was Matlab which I had used before. In this aspect the work included to get familiarized with the simulations that were provided and to learn new tools of the program. For the writing part I used \LaTeX which I'd never used before, but learning how to use it was easy and It provided me a lot of tools in scientific writing.

During the development of the project I confirmed that the school provides me the basic tools that are going to be useful to face the different problems in the work environment but at the end the personal disposition, the dynamism and the open mind to new concepts made this process more useful. While going through this experience I had the opportunity of getting an idea of how the interaction between Industry and research works. It has been so far an

opportunity that has given to me many reasons to want to keep working in the research field.

In general the experience within the radar group at University of Helsinki was an experience that allowed me to improve my skills in different areas: starting from the insertion in a work environment and organization of my time followed by adoption and application of new technical and theoretical concepts, ending in the progress of the basic communications tools (reading, writing and oral expression) in English.

Appendix A

Range resolutions constants

Here is presented the time resolution constant T_{res} defined by Pebbles in [5].

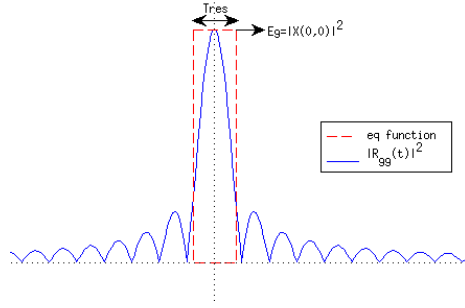


Figure A.1: *Ambiguity function cut*

Figure A.1, shows the ambiguity function cut for some waveform. The time resolution constant t_{res} is defined as the width of a rectangular function equivalent in amplitude and area to the cut. So T_{res} can be defined as in equation A.1 that can be taken as a measure of the range resolution.

$$T_{res} = \frac{\int_{-\infty}^{+\infty} |\chi(\tau, 0)|^2 d\tau}{|\chi(0, 0)|^2} \quad (\text{A.1})$$

There are some alternative forms presented in A.2 and A.3. R_{gg} is the auto-correlation function, E_g is the energy of the complex envelope $g(t)$ and $G(\omega)$ is the fourier transform of $g(t)$.

$$T_{res} = \frac{\int_{-\infty}^{+\infty} |R_{gg}(\tau)|^2 d\tau}{E_g^2} \quad (\text{A.2})$$

$$T_{res} = \frac{\int_{-\infty}^{+\infty} |G(\omega)|^4 d\omega}{2\pi E_g^2} \quad (\text{A.3})$$

So the waveforms for which T_{res} is small can be interpreted as having good resolution. So by using a wideband signal with a given energy small t_{res} can be achieved but this is not enough to assure good resolution because if two targets

are close enough and one of them is larger in amplitude the sidelobes of this target can cause the no detection of the small amplitude target. Because it is important then to note that the resolution depends on how separated are the targets and it is improved as long as the separation between the targets is larger compared to the value of T_{res} .

The effective bandwidth will be then $B_{eff} = \frac{1}{T_{res}}$

For a linear frequency modulated pulse defined by 2.38 and whose $G(\omega)$ is given by A.4 [5]

$$G(\omega) \approx A \sqrt{\frac{2\pi}{\mu}} \text{rect} \left(\frac{\omega}{\mu\tau} \right) e^{-j(\frac{\omega^2}{2\mu} - \frac{\pi}{4})} \quad (\text{A.4})$$

The values for T_{res} and B_{eff} are the followings

$$T_{res} = \frac{2\pi}{\mu\tau} \quad (\text{A.5})$$

$$B_{eff} = \frac{\mu\tau}{2\pi} \quad (\text{A.6})$$

Appendix B

Taylor coefficients

In this part is illustrated the procedure to determine the Taylor's coefficients under the constrains of sidelobe level SLL and number of sidelobes on each side of the main lobe that are constant \bar{n} before the sidelobes start to decrease. This procedure is taken from [5] in chapter number 3 The procedure is the following:

1. Choose SLL which corresponds to the maximum sidelobe level
2. Determine A from equation B.1

$$A = \frac{1}{\pi} \cosh^{-1} \left(10^{\frac{-SLL}{20}} \right) \quad (\text{B.1})$$

SLL in dB, and have to be a negative number.

3. Choose a value for \bar{n}^1
4. For the \bar{n} chosen calculate the beamwidth factor σ_T from equation B.2

$$\sigma_T = \frac{\bar{n}^2}{A^2 + (\bar{n} - 0.5)^2} \quad (\text{B.2})$$

5. Finally the Taylor coefficients are given by the expression B.3

$$f_m = \begin{cases} \frac{(-1)^m \prod_{n=1}^{\bar{n}-1} \left[1 - \frac{m^2 \sigma_T^{-2}}{(A^2 + (\bar{n} - 0.5)^2)} \right]}{2 \prod_{n=1, n \neq m}^{\bar{n}-1} \left[1 - \left(\frac{m}{n} \right)^2 \right]} & m = 1, 2, \dots, (\bar{n} - 1) \\ 0 & m \geq \bar{n} \end{cases} \quad (\text{B.3})$$

¹Usually is the n_{min} defined by Taylor in [26], but can also be a value greater than n_{min}

Appendix C

Zac transform of the transmitted signal

The Zac transform is defined as in [29]. Assuming that the function $f \in L^2(R)$ is known. The Zac transform $Z_f f(t)$ is the representation such that $Z_f : f \rightarrow Z_f f(t) \in L^2_1(R^2)$ and $\forall x, y \in (0, 1)$ the relation C.1 is guaranteed.

$$Z_f(x, y) = \sum_{k=-\infty}^{+\infty} f(x+k)e^{-j2\pi ky} \quad (\text{C.1})$$

Taking into account the expression for the radar ambiguity function studied in section 2.4.2 and C.1 it is easy to show that if $\tau, \omega_d \in Z$ then

$$\chi_f(\tau, \omega_d) = \int_0^1 \int_0^1 |Z_f(x, y)|^2 e^{-j2\pi(\omega_d x + \tau y)} dx dy \quad (\text{C.2})$$

Using periodic function based on the k-th chebyshev polynomial, the Zac transform for the transmitted signal $s(t)$ is

$$Z_f(x, y) = e^{2kpi\|(x,y)\|_p} \quad (\text{C.3})$$

where $\|(x, y)\|_p = (x^p + y^p)^{\frac{1}{p}}$ is the P-norm.

Under these assumptions and the periodicity of the Zac transform the phase $\phi(t)$ can be written as

$$\phi(t) = (k^{p'} - t^{p'})^{\frac{1}{p'}} \quad (\text{C.4})$$

with $t \in (-k, k)$ and $p' = \frac{p}{p-1}$

By limiting t in the interval $(0, \tau)$ and looking for an increasing instantaneous frequency and a causal signal the phase ϕ is expressed as the following

$$\phi(t) = k - \left[\left(t - \frac{\tau}{2} \right)^{p'} \right]^{\frac{1}{p'}} \quad (\text{C.5})$$

so the instantaneous frequency is

$$\omega_i(t) = \frac{t - \frac{\tau}{2}}{\sqrt{k^2 - \left(t - \frac{\tau}{2} \right)^2}} \quad (\text{C.6})$$

Appendix D

Networks and radar signals

D.1 Analytic radar signal

Considering the specific case of pulsed radar the spectrum of the signal $s(t)$ in 2.2 is the one shown in the figure D.1.

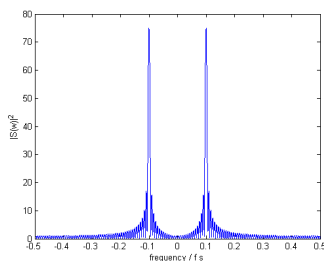


Figure D.1: *Spectrum of pulsed radar transmitted signal*

As one can see the real signal $s(t)$ has a spectrum with both negative and positive frequency components. The negative components can be removed without any loss of information while making mathematical manipulations easier.

In order to take advantage of this characteristic the analytic radar signal is defined as a complex signal chosen to force the spectrum to be 0 $\forall w < 0$ as it is depicted in figure D.2.

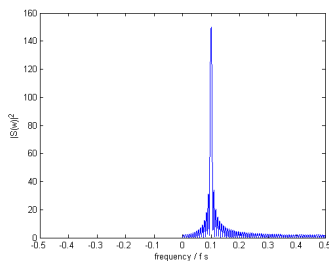


Figure D.2: *Spectrum of pulsed radar analytic transmitted signal*

The analytic signal $\Psi(w)$ can be defined in frequency domain as in D.1

$$\Psi(w) = 2U(w)S(w) \quad (\text{D.1})$$

The real radar signal $s(t)$ in terms of the analytic signal is

$$s(t) = \text{Re}[\psi(t)] \quad (\text{D.2})$$

On the other hand, the radar waveform considered in 2.2 can be written as

$$S(t) = \frac{1}{2} \left(g(t)e^{i(w_0 t + \phi_0)} + g^*(t)e^{-i(w_0 t + \phi_0)} \right) \quad (\text{D.3})$$

Where $g(t)$ is the complex envelope of $s(t)$.

The analytic signal $\psi(t)$ in terms of the complex envelope $g(t)$ is

$$\psi(t) = g(t)e^{j(w_0 t + \phi_0)} \quad (\text{D.4})$$

From this it is evident that the complex envelope $g(t)$ is defined by

$$g(t) = a(t)e^{j\theta(t)} \quad (\text{D.5})$$

It is important to mention that the energy of the analytic signal has twice the energy of the real signal.

D.2 Networks

In radar the passage of the signals through linear networks offers many advantages in the processing of the signal in the receiver. A signal, real or analytic, can be either applied to a real or an analytic network and its response is given by the convolution operation between the signal and the impulse response of the filter. Figure D.3 illustrates four different cases.

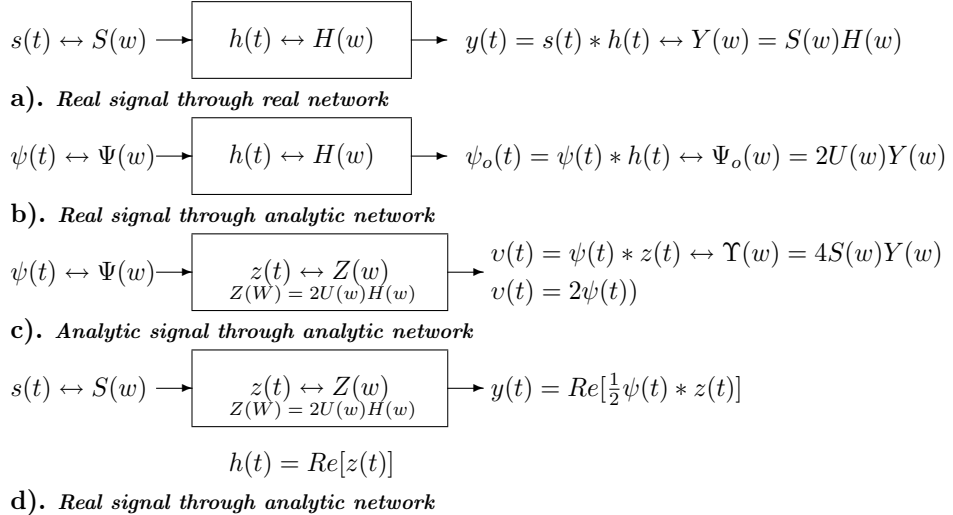


Figure D.3: Signals and networks

Bibliography

- [1] Leslie Lamport, *L^AT_EX: A Document Preparation System*. Addison Wesley. Massachusetts, 2nd Edition, 1994.
- [2] *521-2002 IEEE Standard Letter Designations for Radar-Frequency Bands*. <http://ieeexplore.ieee.org/servlet/opac?punumber=8332>, 2003.
- [3] V.N. Bringi and V. Chandrasekar, *Polarimetric Doppler Weather Radar: principles and applications*. Cambridge University press. New York, 2005.
- [4] B.M. Mahafza, *Radar Systems Analysis and Design using MATLAB*. Chapman and Hall/CRC. USA 2000.
- [5] P.Z. Peebles, Jr, *Radar principles*. Jhon Wiley and Sons, Inc. USA 1998.
- [6] R. H. Barker, *Group Synchronization of Binary Digital Systems*. In Communication Theory. Academic Press, Inc. London, England 1953.
- [7] T. Misaridis and J. A. Jensen, *Use of Modulated Excitation Signals in Medical Ultrasonod. Part I: Basic Concepts and expected Benefits* IEEE Transactions on ultrasonics, ferroelectrics and frequency control. Vol: 52. N_o : 2 February 2005
- [8] A.S. Mudukutore, V. Chandrasekar and R.J. Keeler, *Pulse Compression for Weather Radars* IEEE Transactions on geoscience and remote sensing Vol: 36. N_o : 1 January 1998
- [9] V. Chandrasekar, V.N. Bringi and P.J. Brockwell, *Statistical Properties of Dual-Polarized Radar Signals* Proc. 23rd AMS Conf. Radar Meteorology, Snowmass, Colorado pp:193-196. September 1986
- [10] M.R. Ducoff and B. W. Tietjen, *Radar Hand Book* Mac Graw Hill. USA 3rd Edition, 2008
- [11] R.W. Fetter, *Radar Weather performance enhanced by pulse compression* Prints. 14th AMS Conf. on radar meteorology pp: 413-418. November 1970
- [12] R.W. Gray and D.T. Farley, *Theory of incoherent-scatter measurements using compressed pulses* Radio Sci. Vol: 8. N_o : 2 February 1973
- [13] R.J. Keeler and R.E. Passarelli, *Signal processing for Atmospheric Radars* National Center for atmospheric research note. Boulder. Colorado May 1989

- [14] Y.P. Grihin and A.Zankiewicz, *A neural Network Sidelobe Suppression Filter for a Pulse-compression Radar with Powers-of-Two Weights* 10th Mediterranean Electrotechnical Conference, MEleCon 200, Vol:2 2000
- [15] J. Yang and T.K. Sarkar, *A novel Doppler-tolerant polyphase codes for pulse compression based on hyperbolic frequency modulation* Digital Signal Process 2006
- [16] Nitin Bharadwaj *Simulation of received signal from weather.Radar and Communication Group.* Electrical and Computer Engineering. Colorado State University. Fort Collins CO 80523, 2004
- [17] R. J. Doviak and D. Zrnić , *Doppler radar an weather observations* Dover publications, INC. Mineola New York 2nd Edition, 1993
- [18] M.I. Skolnik, *Radar Handbook* Mac Graw Hill.USA 2rd Edition, 1990
- [19] T. Puhakka¹, P. Puhakka¹, and F. OHora, *On the Performance of NLFM Pulse Compression with Polarimetric Doppler radar* Proceedings of the 4th European Radar Conference. September 2006
- [20] T.Collins and P. Atkins, *Non linear frequency modulation chirps for active sonar* IEE proc. Radar, Sonar Nav. December 1999
- [21] S. Boukeffa, Y. Jiang, T. Jiang, *Sidelobe reduction with Nonlinear Frequency Modulated waveforms* Harbin Engineering University Harbin, CHINA.
- [22] E. Fowle, *The design of FM pulse compression signals* IEEE Transactions on Information Theory. Jan 1964
- [23] E. Cook, *A Class of nonlinear FM pulse compression signals* Proceedings of the IEEE. Nov 1964
- [24] P.C Brandon , *Design of a nonlinear pulse compression system to give a low loss high resolution radar performance* Marconi. 1973
- [25] M. Luszczuk, *numerical evaluation of ambiguity function forstepped non linear FM radar waveform* Conference on microwaves, Radar and wireless. 2006
- [26] T. Taylor, *Design of Line-source antennas for narrow beamwidth and low sidelobes* IRE transactions on antennas and propagation. January 1995
- [27] P.Lynch *The DolphChebyshev window: A simple optimal filter* Met Eireann, Dublin, Ireland. January 1996 and June 1996
- [28] A. Nowicki,W. Secomski, J.Litniewski, I. Trots *On the application of signal compression using Golay's codes sequences in ultrasound diagnostic* Institute of fundamental technological research Plosih academy of sciences. Warszawa,Poland. 2003
- [29] C. Leśnik *Nonlinear Frequency Modulated Signal Design* Military University of Technology, Gen. S. Kaliskiego 2, 00-908 Warszawa, Poland 2009